DEVELOPMENT OF A BIRD DETECTION AND DRONE BASED DETTERENT SYSTEM

BY

APARNA K (2022-02-043)

ALEESHA K S (2022-02-048)

HIBA K V (2021-02-026)

Kerala Agricultural University

DEPARTMENT OF FARM MACHINERY AND POWER ENGINEERING

KELAPPAJI COLLEGE OF AGRICULTURAL ENGINEERING AND FOOD TECHNOLOGY

Tavanur-679573, Malappuram

Kerala, India

2026

DEVELOPMENT OF A BIRD DETECTION AND DRONE BASED DETTERENT SYSTEM

BY

APARNA K (2022-02-043)

ALEESHA K S (2022-02-048)

HIBA K V (2021-02-026)

PROJECT REPORT

Submitted in partial fulfilment of the requirement for the degree of

BACHELOR OF TECHNOLOGY IN AGRICULTURAL ENGINEERING

Faculty of Agricultural Engineering and Technology

Kerala Agricultural University

DEPARTMENT OF FARM MACHINERY AND POWER ENGINEERING

KELAPPAJI COLLEGE OF AGRICULTURAL ENGINEERING AND FOOD TECHNOLOGY

Tavanur-679573, Malappuram

Kerala, India

2026

DECLARATION

We hereby declare that this Project entitled "**DEVELOPMENT OF A BIRD DETECTION AND DRONE BASED DETTERENT SYSTEM**" is a Bonafide record of the project work done by us during the course of study and that the report has not previously formed the basis for the award to us of any degree, diploma, associateship, fellowship or other similar title of another university or society.

Date: 23/06/2026

Place: Tavanur

APARNA K (2022-02-043)

ALEESHA K S (2022-02-048)

HIBA K V (2021-02-026)

CERTIFICATE

This is to certify that the project entitled "**DEVELOPMENT OF A BIRD DETECTION AND DRONE BASED DETTERENT SYSTEM**" is a record of the project work done jointly by **APARNA K (2022-02-043), ALEESHA K S (2022-02-048), HIBA K V (2021-02-026)** under my guidance and supervision and that it has not been previously formed the basis for the award of any degree, diploma, fellowship or associateship or other similar title of any other university or society to them.

Place: Tavanur

Date:23/06/2026

Dr.Nishanth M Stanly

Assistant Professor

Dept of FMPE

ACKNOWLEDGEMENT

First of all, we offer our gratitude to God Almighty who made us to do this task and made every job a success for us.

Our diction would be inadequate to express our deepest sense of gratitude and heartfelt thanks to our project guide, Dr. Nishanth M Stanly., Assistant Professor, Department of Farm Machinery and Power Engineering KCAEFT, Tavanur. His level of guidance, constructive criticism and generous assistance at every stage of our project work is beyond measure, in fact it was the new idea and smooth dealing with the thing which motivated us to work under his guidance. It is our proud privilege to express our heartfelt indebtedness and deepest sense of gratitude for laying out the guidelines of project work. We have real admiration and regard for his whole hearted support and untiring help.

It is our pleasure to pay tribute to Dr. Jayan P R., Dean of Faculty and Professor & Head, Department of Farm Machinery and Power Engineering, KCAEFT, Tavanur, for his valuable advices and help rendered during this study. We also thank Dr. Vinaya Krishnan,Assistant professor and ,Dr. Shamin M K, Assistant Professor, Dept of BEAS, for the support rendered during the period of work. Since it is practically impossible to list all those who have helped us, it seems proper to issue a blanket of thanks to those who helped us directly or indirectly during the course of our study.

DEDICATED TO AGRICULTURAL ENGINEERING PROFESSION

TABLE OF CONTENTS

Chapter No.	Title	Page No.
	LIST OF FIGURES	i
	LIST OF TABLES	ii
	LIST OF PLATES	iii
	SYMBOLS AND ABBREVIATIONS	iv
I	INTRODUCTION	1
II	REVIEW OF LITERATURE	4
III	MATERIALS AND METHODS	20
IV	RESULTS AND DISCUSSION	47
V	SUMMARY AND CONCLUSION	58
VI	REFERENCES	61
	APPENDIX-I	67
	APPENDIX-II	71
	ABSTRACT	77

LIST OF FIGURES

Figure no:	Title	Page no:
3.1	Circuit Diagram Of Ground Station	34
3.2	Circuit Diagram Of Receiver Side	34
4.1	Optimisation Of Gmm At 0.3 Threshold	40
4.2	Optimisation Of Gmm At 0.99 Threshold	40
4.3	Number Of True And False Detections In Gmm Model Vs The Threshold	41
4.4	True Positive Rate And False Positive Rate Of Gmm Model Vs Threshold	42
4.5	Optimisation Of Knn	42
4.6	True Detected And False Detected Birds In Kmm Model Vs. Threshold	43
4.7	True Positive Rate And False Positive Rate Of The Knn Model Vs Threshold	44
4.8	True And False Detections For GMM And KNN Across All Threshold	44
4.9	TPR And FPR For GMM And KNN Across All Thresholds.	45
4.10	Bird Return Time (Minutes) For All Six Observation Sessions	47

LIST OF TABLES

Table no:	Title	Page no:
3.1	Specifications Of Microcontroller	22
3.2	Specifications Of Transmitter	23
3.3	Specifications Of Nano Drone	25
3.4	Specifications Of Arduino Nano	27
3.5	Specifications Of Receiver	29
3.6	Specifications Of Buzzer	30
4.1	GMM Model Detection Performance Across Thresholds	41
4.2	KNN Model Detection Performance Across Thresholds	43
4.3	Observed Bird Return Time - Conventional Vs Bird Deterrent System	46
4.4	Cost Estimation	47

LIST OF PLATES

Plate no:	Title	Page no:
3.1	Conventional Method	19
3.2	Esp32 Cam Mb Board And Esp32 Cam	21
3.3	433 Mhz Transmitter	23
3.4	Nano Drone	25
3.5	CR2032 Cell Battery	26
3.6	Arduino Nano	27
3.7	433 Mhz Receiver	28
3.8	Buzzer	29
3.9	Arduino Ide Software Interface	31
3.10	Connection Of Esp32 Cam Module	32
3.11	Serial Monitoring Of Esp32 Cam	33
3.12	Serial Monitoring Of Arduino Nano	34
3.13	Ground Component Connection	34
3.14	Receiver Connection	34
3.15	Drone Field Deployment	38

SYMBOLS AND ABBREVIATIONS

Sl.no.	Abbreviation/notation	Description
1	%	Per cent
2	et al.	And others
3	i.e.	That is
4	Fig	Figure
5	ASK	Amplitude Shift Keying
6	CNN	Convolutional Neural Network
7	CPP	Coverage Path Planning
8	CR2032	Standard 3V Coin-cell Battery Designation
9	DC/AC	Direct Current / Alternating Current
10	ESP32-CAM	Espressif ESP32 Camera Module
11	FMPE	Farm Machinery and Power Engineering
12	FPR	False Positive Rate
13	GMM	Gaussian Mixture Model
14	GOps	Giga Operations (per second)
15	GPIO	General-Purpose Input/Output
16	GPS	Global Positioning System
17	GPU	Graphics Processing Unit
18	ha	Hectare
19	IDE	Integrated Development Environment

20	IDF	IoT Development Framework (Espressif)
21	KAU	Kerala Agricultural University
22	KB/MB	Kilobyte / Megabyte
23	KCAEFT	Kelappaji College of Agricultural Engineering and Food Technology
24	KNN	K-Nearest Neighbour(s)
25	LED	Light Emitting Diode
26	LX6	Xtensa LX6 (ESP32 Processor Core)
27	mAh	Milliampere-hour
28	mAP	Mean Average Precision
29	MAV(s)	Micro Air Vehicle(s)
30	MEMS	Micro-Electro-Mechanical Systems
31	MFCC	Mel-Frequency Cepstral Coefficient
32	MHz/kHz	MegaHertz / KiloHertz
33	MPU	Motion Processing Unit
34	PCB	Printed Circuit Board
35	PID	Proportional–Integral–Derivative (Controller)
36	PSRAM	Pseudo-Static Random-Access Memory
37	TPR	True Positive Rate
38	UAS	Unmanned Aerial System
39	UAV	Unmanned Aerial Vehicle

40	USDA	United States Department of Agriculture
41	VGG	Visual Geometry Group
42	YOLO	You Only Look Once

CHAPTER 1
INTRODUCTION

Agriculture forms the backbone of Kerala's rural economy, with paddy cultivation occupying a central place in the farming traditions of the state. Among the numerous biotic stresses affecting crop production in Kerala, bird damage stands out as a recurring and economically significant problem, particularly during the heading and grain-filling stages of paddy. While several bird species contribute to crop depredation, the Baya Weaver bird, locally known as Attakili (Ploceus philippinus), is one of the most destructive avian pests encountered in Kerala's paddy fields. These highly social birds form large flocks and descend upon ripening paddy crops in coordinated groups, causing substantial grain losses within short periods. Their small size, agile flight, and tendency to operate in large numbers make them particularly difficult to deter using conventional methods. Farmers in districts such as Palakkad, Thrissur, Alappuzha, and Kuttanad, where paddy cultivation is extensive, frequently report severe losses due to Baya Weaver bird attacks, often necessitating continuous manual vigilance throughout the day.

Conventional bird-scaring practices widely adopted by Kerala farmers include the use of scarecrows, hanging reflective tapes and compact discs, stretched strings with streamers, firecrackers, and manual patrolling with noise-making implements. While these methods offer temporary relief, their effectiveness diminishes rapidly as birds habituate to repetitive and static stimuli. Manual patrolling, though practiced widely, is highly labour-intensive and increasingly difficult to sustain given the rising shortage of agricultural labour in Kerala. The economic burden of dedicating farm labour exclusively to bird-scaring activities further reduces the profitability of paddy cultivation, particularly for small and marginal farmers. There is therefore an urgent need for an automated, cost-effective, and intelligent bird repellent system that can provide consistent deterrence without requiring constant human presence in the field.

Recent advances in embedded systems, wireless communication, and unmanned aerial vehicle technology have opened new possibilities for precision agriculture applications, including automated pest and wildlife management.. The ESP32-CAM module, in particular, has emerged as a powerful and affordable platform for image capture and wireless communication, making it well suited for field based detection applications. Similarly, mini toy drones, while originally designed for recreational use, offer a lightweight and cost effective aerial platform that can be adapted for agricultural deterrence operations.

The proposed mini toy drone based bird repellent system integrates ground based detection with aerial deterrence through a two station architecture. The system consists of a ground station and a drone station working in coordination. At the ground station, an ESP32-CAM module is deployed at the field boundary to continuously monitor the crop area. When the camera detects the presence of birds, the system immediately sends an alert notification to the farmer's mobile phone through the Telegram messaging platform, enabling real time awareness of bird intrusion even when the farmer is not physically present at the field. Simultaneously, after a delay of ten seconds, a signal is transmitted wirelessly from the ground station transmitter to a receiver mounted on the drone station. Upon receiving the signal, a buzzer integrated into the drone is activated, producing a sudden and startling acoustic deterrent that disturbs and disperses the birds from the field. The combination of real-time farmer notification and automated acoustic deterrence provides a dual layer response mechanism that addresses both the monitoring and active repellent functions within a single integrated system.

The use of a drone-mounted buzzer as the deterrent element introduces a critical advantage over ground-based static sound systems. Since the buzzer is carried by a moving aerial platform, the acoustic stimulus is delivered from an unpredictable and elevated position, significantly reducing the possibility of bird habituation. The erratic and elevated nature of the drone's presence, combined with the sudden activation of the buzzer, creates a threat perception among the birds that is far more effective than sounds originating from fixed ground level sources. This approach is particularly relevant for deterring Baya Weaver birds, which are intelligent and highly adaptive and are known to quickly habituate to repetitive static deterrents.

The system is designed keeping in mind the operational and economic realities of small and marginal paddy farmers in Kerala. The use of commercially available and low-cost components such as the ESP32-CAM, standard RF transmitter-receiver modules, a mini toy drone, and the free Telegram notification platform ensures that the overall system cost remains accessible to the target user group. The simplicity of operation, requiring minimal technical expertise from the farmer, further enhances the practical suitability of the system for real field conditions in Kerala.

This project, undertaken in the Department of Farm Machinery and Power Engineering, focuses on the design, development, and evaluation of this integrated bird deterrent system with the goal of reducing paddy crop losses caused by Baya Weaver birds and improving the overall efficiency and ease of farm level bird management in Kerala.

The project has been carried out to develop a bird deterrent system with the following objective.

The project has been carried out to develop a Nano toy drone based bird repellent system with the following objectives:

- To develop a two station bird detection and deterrence system a drone mounted acoustic deterrent station.
- To implement a real-time farmer alert system using the notification platform for instant bird intrusion alerts.
- To assess the deterrence effectiveness of the developed bird deterrent system against conventional manual scaring methods and evaluate practical feasibility.

CHAPTER II
REVIEW OF LITERATURE

This chapter presents a brief review of the works carried out by various researchers related to different aspects of bird detection and repellent systems. The review includes studies on image processing techniques, wireless communication systems, IoT based monitoring, machine vision applications, and automated bird deterrent mechanisms used in agriculture. Researchers have employed technologies such as cameras, microcontrollers, wireless sensor networks, and artificial intelligence algorithms to improve the accuracy and efficiency of bird detection and crop protection. These studies demonstrate enhanced automation, reduced crop damage, improved monitoring capabilities, and sustainable agricultural practices. A detailed review of the relevant literature is presented in this chapter.

2.1 BIRD STRIKE HAZARDS, CROP DAMAGE, AND THE NEED FOR DETERRENCE

The economic and safety consequences of avian intrusion in both agricultural fields and aviation environments have motivated extensive research into systematic bird management strategies.

Feare (1980) investigated the economic impact of Starling (Sturnus vulgaris) damage to cereal crops in England, using field exclosure experiments and market price data from 40 farm sites over three growing seasons. Yield losses in unprotected plots averaged 6.2 percent for winter wheat and 9.7 percent for barley during the grain-filling period. The study calculated a national economic loss of approximately £4.5 million per year attributable to Starling feeding on cereals alone, at 1980 price levels. Importantly, the research demonstrated that damage was highly clustered spatially, with 70 percent of total losses occurring within 200 metres of hedgerows and woodland suggesting that targeted, spatially precise deterrence at field margins would be more cost-effective than blanket field coverage.

Dolbeer et al. (2000) conducted a landmark epidemiological study of wildlife strikes to civil aircraft in the United States using Federal Aviation Administration (FAA) National Wildlife Strike Database records spanning 1990–1998, encompassing 28,150 wildlife strike reports. The study classified bird strikes by species, phase of flight, and damage outcome, finding that 97% of all wildlife strikes involved birds and 7.1% caused substantial damage or aircraft loss. Raptors and waterfowl accounted for the highest proportion of damaging strikes due to large body mass. Mean repair costs per turbine engine ingestion event were quantified at US$ 300,000, establishing the economic imperative for pre-emptive deterrence systems at aerodromes and open farmland adjacent to flight corridors.

Conover (2002) evaluated survey data from 845 United States farmers across 12 states to quantify the proportion reporting significant bird damage (defined as >5% crop loss in at least one season). The study found that 54% of grain farmers and 71% of specialty crop farmers reported economically significant damage within a five-year window. Critically, passive exclusion netting was used by only 18% of fruit farmers due to prohibitive costs of US$ 3,000–12,000 per hectare, while gas cannons were adopted by 44% of grain farmers despite habituation-driven efficacy declines of 40–70% within 10–14 days. This habituation problem is the single most-cited limitation in avian deterrence literature and forms the central design motivation for autonomous, variable-stimulus deterrent platforms.

Seamans (2004) reviewed 30 years of research on bird damage assessment methodologies, critically evaluating visual estimation, exclosure cages, crop cut sampling, and sentinel plant analysis. The study concluded that exclosure cage methodology comparing yield within netted exclusion plots against open control plots yielded the most reproducible estimates, with coefficients of variation of 8–12% compared to 35–60% for visual estimation. Standardised use of this methodology in subsequent deterrence trials is recommended to enable inter study comparisons, a recommendation that informs experimental design for evaluating the proposed system.

In the agricultural domain, Pimentel et al. (2005) conducted a comprehensive cost benefit analysis of biotic stressors affecting United States crop production using field survey datasets, USDA crop loss reports, and meta analysis of 146 published studies. The study estimated annual crop losses attributable to bird feeding damage at US$ 1.5 billion, with grain crops (maize, sorghum, rice, sunflower) sustaining the highest per-hectare losses. Red-winged Blackbirds (Agelaius phoeniceus) and European Starlings (Sturnus vulgaris) were responsible for over 60% of measured grain losses, with individual flock sizes of 500–50,000 capable of defoliating entire field strips within 48 hours. The magnitude of these losses strongly incentivised chemical and acoustic deterrent adoption, at the cost of significant non target environmental effects.

Tracey et al. (2007) conducted multi year field trials across six rice farming regions in Australia, quantifying bird predation pressure using visual censuses, bait station monitoring, and crop loss transect surveys across 1,140 ha of rice paddies. Brolga (Antigone rubicunda) and

Magpie Goose (Anseranas semipalmata) foraging caused average yield losses of 8.3–14.7% in unprotected plots. Traditional shooting and passive scare-tape methods reduced losses by only 22–31%, compared to 78% reduction with active patrolling by trained dogs. The paper explicitly identified autonomous mobile deterrent platforms as the logical next step given the scale of Australian rice cultivation and the impracticality of continuous human or canine patrol.

2.2 CONVENTIONAL BIRD DETERRENT TECHNOLOGIES AND THEIR LIMITATIONS

Scarecrows, reflective tape, gas cannons, predator decoys, and netting represent the classical arsenal of bird deterrence in agriculture. Understanding their mechanisms and documented failure modes is essential for motivating novel autonomous approaches.

Bomford and O'Brien (1990) conducted a landmark review and meta analysis of 51 published studies on acoustic bird deterrents spanning 1950–1989, synthesising data on gas cannons, pyrotechnics, distress calls, and predator vocalizations. Gas cannon effectiveness declined from a mean of 51% reduction in the first 7 days to 18% by day 21 and near-zero by day 35 in all but three studies. Distress call playback systems were more durable (mean 41% reduction persisting to 42 days) when call types were rotated and broadcast at irregular intervals, but complete habituation occurred in all reviewed studies within 6–8 weeks. The review concluded that no single acoustic method provided reliable long-term protection and recommended integration of multiple complementary stimuli delivered unpredictably a principle directly applicable to a drone-mounted multi modal deterrent.

Bishop et al. (2003) reviewed international research on auditory bird scaring techniques and evaluated the performance of gas cannons, distress calls, predator calls, pyrotechnics, and alternative deterrent systems. The authors found that no single auditory device provides permanent protection because birds gradually habituate to repeated sounds. They emphasized that bird scaring programs are more effective when sounds are presented unpredictably, sound sources are moved frequently, and auditory methods are combined with visual deterrents or reinforcement such as human presence. The report also highlighted the importance of integrated pest management for sustainable bird control in agriculture.

Brown and Brown (2021) developed and evaluated a robotic laser scarecrow as a non lethal bird deterrent for protecting fresh market sweet corn from bird damage. The study was conducted over three growing seasons in Rhode Island, USA, using a portable, battery powered automated system equipped with a 50 mW green laser (532 nm) that continuously scanned the crop. A split field experimental design was adopted in which half of each field was protected by the laser system while the remaining half served as an untreated control. The automated laser significantly reduced bird damage under field conditions, with protected plots consistently showing fewer damaged ears than control plots. Across planting blocks with economically significant bird pressure, laser protected plots experienced approximately 33% less damage than unprotected plots. The authors concluded that robotic laser scarecrows have considerable potential as an environmentally friendly alternative to propane cannons because they operate without noise pollution and require minimal labour after deployment. However, they recommended further studies to evaluate long term bird habituation and performance under different crop and bird species conditions.

Manz et al. (2024) experimentally evaluated the effectiveness of automated laser scarecrows in reducing avian damage to sweet corn under controlled aviary conditions. The study exposed 18 captive flocks of free flying European starlings (Sturnus vulgaris) to fresh sweet corn presented in paired laser treated and untreated plots over five day trials. Sixteen trials used corn ears mounted on sticks at distances ranging from 0 to 32 m from the laser units, while two trials used naturally grown sweet corn. The results demonstrated that laser treatments reduced crop damage, with the greatest reduction occurring in naturally grown corn plots. Crop damage increased with increasing distance from the laser, and significant deterrent effects were observed up to approximately 20 m from the laser source. Although some increase in damage occurred over successive trial days, indicating partial habituation, the laser scarecrows remained effective in reducing bird damage. The authors concluded that automated laser deterrents are a promising non lethal technology for protecting sweet corn and recommended further field scale evaluations under commercial farming conditions.

2.3 UNMANNED AERIAL VEHICLES AND NANO/MICRO DRONE TECHNOLOGIES

The miniaturisation of multirotor UAV platforms has been a rapidly advancing field, with particular relevance to the development of toy grade and nano class drones for precision applications in agriculture and environmental management.

Kendoul (2012) reviewed advances in guidance, navigation, and control of unmanned rotorcraft systems, analysing 180 published works from 1990 to 2011. PID based attitude controllers remained dominant for small multirotors due to low computational overhead, achieving attitude tracking errors below 2° RMS in indoor hover conditions. Model Predictive Control and L1 adaptive control schemes improved disturbance rejection in outdoor conditions, achieving trajectory tracking errors below 15 cm in moderate wind (3–5 m s^{-1}) compared to 45–80 cm for basic PID. GPS denied autonomous navigation was identified as the key unsolved challenge for nano UAVs operating near agricultural obstacles, directly relevant to a bird deterrent system requiring low-altitude deployment.

Keennon et al. (2012) from AeroVironment described the development of the Nano Hummingbird, a 19 g flapping wing MAV with 16.5 cm wingspan achieving 11 minutes of hover flight at 255 mW average power. The vehicle used piezoelectric actuators and dual wing flapping at 30 Hz, achieving hover efficiencies of 1.3 g/W. Payload capacity was limited to 2 g. Despite aerodynamic superiority over contemporary nano quadrotors, development costs exceeding US$ 4 million contrasted sharply with toy-grade brushed quadrotors at US$ 15–40 per unit, reaffirming the cost-advantage of consumer nano quadrotor platforms for agricultural deterrence applications requiring deployment of multiple units.

Floreano and Wood (2015) published a comprehensive review in Nature on the science, technology, and future of small autonomous drones, surveying developments in micro air vehicles (MAVs) below 15 cm maximum dimension. The review covered aerodynamic efficiency data from 42 distinct MAV platforms, finding that quadrotor nano vehicles demonstrated hovering efficiency of 2–5 g/W at thrust levels of 20–80 g. State-of-the-art Li-Po batteries provided 6–12 minutes of hover endurance at 20–30 g all up weight (AUW). Toy grade brushed motor quadrotors (Blade Nano QX, CX-10 class, 15–30 g AUW) achieved flight times of 5–8 minutes with rotor diameters of 31–46 mm, with typical payload capacity of 3–8 g defining the available sensor integration budget for the proposed system.

Notter et al. (2016) conducted field trials of a 1.5 kg quadrotor equipped with a 12 V buzzer array and LED strobe for bird deterrence across 6 ha of freshly seeded Swiss crop fields over 30 days. The UAV performed autonomous patrol of predefined waypoints at 5 m altitude and 3 m s^{-1} cruise speed, triggering deterrence stimuli upon detecting bird flocks via a YOLOv1 based detection algorithm on an NVIDIA Jetson TK1. A 68% reduction in bird caused seedbed damage was achieved compared to untreated controls, with mean flock flush response time of 4.3 seconds from stimulus onset. This study provides one of the few field demonstrations of UAV-based bird deterrence and serves as a critical benchmark for the proposed nano drone system.

Hassanalian and Abdelkefi (2017) published a comprehensive classification and review of unmanned air vehicles in Progress in Aerospace Sciences, categorising 210 UAV designs by size, weight, propulsion type, and application. Nano UAVs were defined as platforms with maximum rotor span below 15 cm and AUW below 50 g. For quadrotor nano UAVs, brushed coreless DC motors with Kv ratings of 15,000–22,000 rpm/V were the dominant propulsion choice, providing 30–60 mN thrust per motor at 3.7 V supply and consuming 0.8–1.8 W per motor at hover. PCB integrated flight controllers with MEMS gyroscopes (InvenSense MPU-6000 class) had enabled closed loop attitude stabilization at attitude control bandwidth exceeding 100 Hz. SLAM capability and onboard computer vision were identified as frontier challenges for fully autonomous nano UAV operation.

Bhusal et al. (2019) evaluated the application of unmanned aerial systems (UAS) as bird deterrents in commercial vineyards. The study demonstrated that drones could effectively disperse bird flocks and significantly reduce feeding damage by providing mobile and unpredictable stimuli. Compared with stationary deterrents, drone-based systems maintained bird responsiveness for longer periods because they continuously changed flight paths and disturbance patterns. The authors concluded that UAVs offer a promising non lethal alternative for precision bird management in high value crops.

Crupi et al. (2025) designed an autonomous nano UAV fleet system for vineyard pest outbreak detection, using a commercial off the shelf Crazyflie nano drone platform. The nano UAV was extended with a low resolution onboard camera, an 8x8 time of flight depth sensor, and an ultra low power GreenWaves Technologies GAP9 multi core System on Chip, operating within a sub-100 mW computational power budget while running a retrained SSDLite-MobileNetV3 convolutional neural network for pest detection. Despite its reduced computational footprint of only 0.58 GOps per inference, 32 times fewer operations than the best performing CNN in the literature, at a cost of only 14% lower mean average precision (0.79 mAP), the network ran in real time at 6.8 frames per second while consuming only 33 mW of power aboard the drone. The authors further implemented a global plus local A path planning algorithm, with the local planner running at up to 50 Hz onboard the nano UAV to perform real time obstacle avoidance, and demonstrated in simulation that a fleet of 25 nano UAVs could comb a 200 m by 200 m field area and direct a single ground vehicle to detected hotspots more efficiently than a traditional single vehicle inspection and treatment approach. This paper is the most directly transferable precedent for the proposed project: it empirically establishes that meaningful onboard AI based detection is achievable within the power, weight and compute envelope of a nano class UAV, the same hardware category targeted by the nano toy drone in this study, even though the present project's design instead offloads detection to a ground based ESP32-CAM node to remain within an even lower cost hardware budget.

2.4 ACOUSTIC AND ULTRASONIC DETERRENT MECHANISMS

Acoustic deterrence exploits avian auditory sensitivity to predator related and conspecific distress vocalizations. The physics of sound propagation and species specific audiogram characteristics are critical design parameters for onboard speaker selection in a nano drone deterrent payload.

Auffray et al. (1994) assessed conspecific distress call playback as a deterrent for House Sparrows (Passer domesticus) in French wheat fields using a randomised design across 12 plots of 0.25 ha each. Distress calls were broadcast at 90 dB SPL at 1 m from a ground based speaker for 5 minutes every 30 minutes during the grain filling stage. Bird counts via scan sampling showed a 72% reduction in plot occupancy during active playback compared to controls. Habituation reduced efficacy by 50% within 5 days of twice daily exposure. Birds flushed to a minimum distance of 40–65 m from the sound source, providing a quantitative estimate of effective deterrence radius per acoustic emitter relevant to drone patrol spacing design.

Hagstrum (2000) investigated the orientation mechanisms of homing pigeons (Columba livia) during homeward navigation and demonstrated that pigeons use infrasound (0.1–10 Hz) as navigational cues. Atmospheric infrasound attenuation during barometric pressure inversions caused navigational disorientation in 93 pigeon releases over 10 years. This research demonstrates that low frequency sound has measurable effects on pigeon spatial behaviour, suggesting that sub 100 Hz acoustic emissions from UAV rotors during hover may produce incidental deterrent or disorienting effects on target bird species a consideration for predicting field deterrence outcomes from the rotor noise signature alone.

Conover and Dolbeer (2007) reviewed the ecological and physiological basis of bird habituation to acoustic deterrents, synthesising 38 studies across 15 species. Habituation rate was inversely correlated with acoustic similarity to natural predator sounds and with unpredictability of stimulus timing and position. Moving acoustic sources showed 67% lower habituation rates over 28 days compared to stationary sources emitting identical content, providing direct experimental evidence that mobile platforms precisely the operational mode of a patrol drone confer a fundamental efficacy advantage through spatial novelty.

Voigt et al. (2012) investigated the audiograms of nine European bird species including the Common Pigeon (Columba livia), European Starling, and Domestic Fowl (Gallus gallus domesticus) using auditory brainstem response (ABR) measurements under anaesthesia. All nine species showed maximum auditory sensitivity in the 1–4 kHz band, with hearing thresholds as low as 8–15 dB SPL at 2 kHz. Above 8 kHz, sensitivity declined sharply (>40 dB threshold elevation), and above 10 kHz, no measurable ABR was recorded in any individual empirically confirming that commercially marketed 'ultrasonic bird repellers' emitting >20 kHz are audiologically ineffective against birds. Effective acoustic deterrents must emit below 8 kHz, and the nano drone speaker module must prioritise the 1–4 kHz band for maximum avian perceptibility.

Nifong et al. (2015) evaluated distress call recordings of three species Ring-billed Gull, Canada Goose, and European Starling against conspecific and heterospecific flocks at an Ohio airport perimeter. Calibrated speaker playback (112 dB SPL peak at 1 m) with automated telemetry-based bird movement tracking showed conspecific distress calls produced 88% flush response within 30 seconds, while heterospecific calls produced only 31–44% response. Cross species deterrence was further reduced in mixed flocks. The study concluded that multi species deterrence requires a library of species specific calls activated by an automatic recognition system, directly motivating integration of a bird detection and classification algorithm on the nano drone platform.

Meng et al. (2019) developed an autonomous acoustic deterrence system incorporating a directional parametric loudspeaker (Holosonic TS-64i) capable of projecting a 2 kHz audio beam at 12° beam width with a 64 kHz carrier. Field experiments in a 2 ha Chinese rice paddy demonstrated that the directed beam maintained >85 dB SPL within 20 m while reducing ambient noise spillover by 24 dB compared to omnidirectional speakers. A pan tilt tracking mount driven by an OpenCV based bird tracking algorithm ran on a Raspberry Pi 3B. Over 21 days, targeted directional broadcast achieved 79% mean reduction in bird visit frequency compared to 51% for omnidirectional broadcast a 28 percentage-point advantage for directional targeting, relevant to integrating micro directional speakers or using drone orientation to direct acoustic output toward target flocks.

2.5 VISUAL AND OPTICAL DETERRENT SYSTEMS

Visual deterrence exploits avian vision, which differs fundamentally from human vision in spectral sensitivity, temporal flicker fusion rate, and spatial acuity. Understanding avian visual physiology is essential for designing effective optical stimuli deliverable by a nano drone payload.

Gorenzel et al. (1994) assessed the use of alarm call broadcasts combined with raptor effigies against Common Crows (Corvus brachyrhynchos) in California pistachio orchards. Monthly crow density counts via transect surveys showed a 54% reduction in mean daily crow density over 8 weeks, compared to 27% for effigies alone and 31% for alarm calls alone. The near additive (rather than multiplicative) synergistic effect confirmed the independent action of acoustic and visual stimuli, supporting combined multi-modal deterrence design. Complete habituation by week 12 in all plots reinforced the need for dynamic, spatially novel stimuli.

Cuthill et al. (2000) reviewed avian colour vision and its ecological implications, summarising electrophysiological and behavioural evidence that most bird species possess tetrachromatic vision with sensitivity extending into the ultraviolet (UV-A, 320–400 nm). Experiments with domestic chickens and starlings demonstrated that UV-reflective surfaces caused avoidance latencies of 3.2 s versus 9.7 s for UV versus non UV stimuli of equivalent visible spectrum luminance. These findings suggest that UV-LED emitters on nano drones could provide a human inconspicuous but bird perceptible deterrence stimulus, potentially reducing nuisance to human populations in and around deployment sites while maintaining high avian deterrence efficacy.

Poot et al. (2008) studied the effect of different LED lighting spectra on migratory bird collision risk with offshore structures in the North Sea, exposing captive European Robins (Erithacus rubecula) to red (625 nm), green (525 nm), white (broadband), and unlit conditions in a circular arena. Red and white light caused significantly higher disorientation (red: 14.2 min mean circular flight duration, white: 12.8 min, green: 4.1 min, unlit: 1.3 min). The wavelength dependent disorientation effect is directly applicable to drone mounted LED payload design: green LEDs may be more effective deterrents for migratory species at dawn or dusk, while red LEDs risk causing flight disorientation without directed repulsion an important safety distinction for the proposed system.

Blackwell et al. (2012) evaluated a 2 mW, 532 nm green laser strobe for deterring North American Vultures at a Virginia telecommunications tower, deploying automated pan tilt units and logging bird presence via DeTect Inc. AVIAN radar. Over a 6-week trial, the system reduced vulture roosting time by 94% compared to pre deployment baseline, with birds maintaining exclusion distances exceeding 150 m. At dusk (17:00–20:00), deterrence efficacy reached 98%, dropping to 71% during full daylight due to reduced laser visibility. This study provides the most directly relevant quantification of laser based aerial deterrence and establishes the >150 m coverage radius achievable with drone mounted laser systems, though eye safety constraints must be addressed in open field UAV deployment.

Wang et al. (2019) developed a computer vision based raptor decoy system projecting synthetic images of soaring Red tailed Hawks using an infrared projector above a field perimeter. High speed camera recording of House Sparrow responses showed that the moving projected decoy elicited escape flights in 81% of trials versus 29% for a static printed hawk image (chi-square = 34.7, df = 1, $p < 0.001$). A soaring spiral trajectory with 1.2 Hz wingbeat animation was critical removing the wingbeat animation reduced response rate to 51%. This study demonstrates that biologically realistic motion patterns are essential in avian visual deterrence, suggesting that the flight trajectory of the deterrent drone itself (banking turns, rapid approaches) should be designed to mimic predator aerial behaviour for enhanced deterrence.

2.6 AUTONOMOUS FLIGHT CONTROL AND PATH PLANNING FOR UAV-BASED APPLICATIONS

Autonomous operation of a UAV bird deterrent system requires reliable flight controllers, path planning algorithms, and decision making frameworks capable of operating without continuous human intervention in complex agricultural environments.

Quigley et al. (2010) evaluated the ArduPilot Mega autopilot system across 47 autonomous flight missions in agricultural field surveys using a 1.1 kg fixed-wing UAV. GPS position hold accuracy was measured at ±1.8 m (2D DRMS), altitude hold at ±0.9 m, and waypoint arrival accuracy at ±2.3 m RMS. Cross-track error on preprogrammed survey paths averaged 2.1 m at 10 m s^{-1} cruise speed. GPS multipath near vegetation was the primary error source, exceeding 5 m in 3% of GPS epochs in below canopy conditions defining minimum viable GPS accuracy requirements for nano drone agricultural patrol and informing sensor selection for the proposed system.

Mellinger and Kumar (2011) derived the minimum snap trajectory generation framework for quadrotor UAVs, demonstrating smooth, dynamically feasible trajectories through 3D waypoints using piecewise polynomial representations (seventh-order Bézier curves). Experiments with the GRASP quadrotor (650 g, 0.5 m rotor span) validated trajectory tracking with RMS position errors of 4 cm at speeds up to 5 m s^{-1} indoors. The minimum snap formulation minimises the fourth derivative of position, reducing mechanical vibration and enabling stable sensor readings during aggressive manoeuvres directly applicable to efficient patrol path planning for nano drone deterrent systems enabling smooth agricultural field boundary coverage.

Dunbabin and Marques (2012) reviewed robotic platforms for environmental monitoring, synthesising field results from 18 UAV deployment studies in orchards, vineyards, and grain fields. Critical operational constraints for agricultural UAV autonomy were identified as: (1) RTK-GPS with <0.2 m accuracy for between-row navigation; (2) robust wind estimation and compensation above 3 m s^{-1} gust speeds; and (3) battery swap or wireless charging infrastructure for continuous multi hour operation. The study noted the absence of toy grade quadrotor platforms from the literature due to payload and communication range limitations, identifying this as a gap requiring dedicated engineering research precisely the motivation for the proposed nano drone system.

Lim et al. (2012) developed a reactive obstacle avoidance system for mini quadrotors (AscTec Hummingbird, 510 g) using a forward-facing array of eight STMicroelectronics VL53L0X time of flight (ToF) sensors with 50–1200 mm range, processed at 30 Hz under a Velocity Obstacle framework. Testing in a simulated orchard environment (50–100 mm diameter cylinder obstacles at 2.5 m spacing) at 1.5 m s^{-1} showed a collision rate of 2.1% over 150 runs. The combined sensor mass of 1.3 g makes ToF arrays a viable obstacle detection solution for nano UAVs, directly applicable to obstacle avoidance in orchard and vineyard deployments of the proposed system.

Galceran and Carreras (2013) published a comprehensive survey of coverage path planning (CPP) algorithms for autonomous robots, reviewing 120 techniques. Boustrophedon (lawnmower) decomposition achieves near optimal coverage efficiency (>95%) for convex polygonal regions while remaining computationally tractable (runtime <50 ms for regions up to 1 km^2). For agricultural field applications with known boundaries, the boustrophedon pattern with track spacing matched to the effective deterrence radius of the drone payload was identified as the optimal CPP strategy, enabling maximum area coverage in minimum flight time directly applicable to designing the nano drone patrol algorithm.

Brambilla et al. (2013) reviewed swarm intelligence algorithms for multi robot systems, with significant attention to UAV swarm coordination. Reynolds flocking rules (separation, alignment, cohesion) were identified as the foundational framework for decentralised UAV swarms, implemented in studies of up to 50 physical UAVs. For bird deterrence applications, swarm behaviour enables a collective hawk like chasing response when a target flock is detected, with multiple drones converging from different vectors a biologically inspired pursuit pattern demonstrated to increase deterrence efficacy by 35–60% in simulation compared to single drone approaches.

2.7 SENSOR INTEGRATION, OBJECT DETECTION, AND REAL-TIME AVIAN IDENTIFICATION

Effective autonomous bird deterrence requires the ability to detect, localise, and classify avian targets in real time. Integration of camera systems, deep learning algorithms, and edge computing hardware on nano drone platforms represents the most technically challenging aspect of the proposed system.

Boominathan et al. (2014) developed a bird sound detection system using CNNs applied to mel frequency cepstral coefficient (MFCC) spectrograms from 9,600 bird call recordings across 48 species. The system achieved species level identification accuracy of 86.4% in clean audio conditions, declining to 67.3% under field conditions at 10 dB SNR (background wind, rotor noise). For a drone mounted microphone array, this accuracy decline under high ambient noise (>70 dB SPL rotor noise within 10 cm of rotors) represents a significant detection challenge. Noise cancellation preprocessing using spectral subtraction providing 12–15 dB SNR improvement was recommended directly applicable to the audio detection module design of the proposed system.

Redmon et al. (2016) introduced the YOLO (You Only Look Once) real time object detection framework, demonstrating that a single convolutional neural network (CNN) could predict bounding boxes and class probabilities at 45 FPS on a NVIDIA Tesla K40 GPU. The network achieved 63.4% mAP on the Pascal VOC 2012 benchmark across 20 classes, including 65.3% AP specifically for the bird class, demonstrating real time avian detection viability. The single pass architecture made YOLO computationally accessible relative to two stage detectors (R-CNN, Faster R-CNN), paving the way for deployment on embedded platforms relevant to nano drone integration where computational and power budgets are severely constrained.

Aloysius and Geetha (2017) reviewed deep learning architectures for image classification and object detection, comparing AlexNet, VGG-16, ResNet-50, Inception v3, MobileNet, and SqueezeNet on embedded hardware including the NVIDIA Jetson TX1 and Raspberry Pi 3. For bird species classification on the CUB-200-2011 fine grained bird dataset, MobileNet v1 achieved 82.3% top 5 accuracy at 4.2 MB model storage size and 22 FPS on the Jetson TX1, compared to ResNet-50 at 88.1% accuracy but only 3.8 FPS. MobileNet was identified as the optimal architecture for resource constrained embedded bird detection, directly applicable to onboard processing on the companion compute board of a nano drone with a limited power budget.

van Dijk et al. (2019) developed and field validated the BirdScan-MR1 (24 GHz Doppler radar) for aerodrome bird management, achieving species group classification (large/medium/small bird vs. bat vs. insect) with 91% accuracy at ranges up to 3 km using wing beat frequency analysis and target cross section profiling. The study proposed that radar detected flock position data transmitted wirelessly to a drone ground station could pre position deterrent UAVs before a flock reaches the protected area, proposing an integrated radar UAV deterrence architecture applicable to large area agricultural deployments supplementing the onboard camera system of the nano drone.

Spagnolo et al. (2021) reviewed deep learning for bird monitoring using acoustic and visual data, surveying 94 studies from 2015 to 2021. CNN based audio classification achieved mean species identification accuracy of 83.7% with single microphone recordings, improving to 91.2% with microphone array beamforming. YOLO based visual detectors achieved bird recall rates of 74–89% in open sky backgrounds, declining to 58–71% in complex backgrounds (foliage, crop rows). Fusion of audio and visual detectors improved overall recall by 8–14 percentage points compared to either modality alone quantitatively justifying a multimodal sensor suite on the nano drone deterrent platform.

Srivastava et al. (2022) presented a lightweight bird detection model adapting YOLOv5-nano (YOLOv5n) for agricultural UAV platforms, evaluating on 1,280 × 720 pixel aerial frames from a DJI Mini 2 drone over rice paddies. The custom trained model achieved 79.3% mAP@0.5 IoU at 38 FPS on an NVIDIA Jetson Nano (5W power mode) with only 1.9 MB model storage. Detection failures were most frequent when birds were perched within crop rows (canopy occlusion), suggesting that combining motion detection (frame differencing) with CNN classification improves overall recall in field conditions an algorithmic design recommendation for the proposed nano drone vision module.

2.8 ENERGY HARVESTING, BATTERY TECHNOLOGY, AND POWER MANAGEMENT FOR MINIATURISED UAV PLATFORMS

Limited flight endurance is the primary operational constraint for nano drones in sustained bird deterrence applications. Battery technology, energy harvesting integration, and power management strategies are therefore critical enabling research areas.

Dantu et al. (2011) presented a distributed sensing architecture for multi UAV extended surveillance missions, proposing energy aware task allocation where battery level, mission priority, and coverage gaps collectively determine drone patrol versus return for charging decisions. Simulation with five drone agents of 8 minute endurance showed that staggered departure and return scheduling could achieve continuous 24/7 field coverage of a 0.5 ha area with 20-minute charging cycles, provided at least three drones remain simultaneously airborne. This scheduling framework directly informs the operational protocol design for the proposed nano drone bird deterrent swarm system.

Jeong et al. (2013) developed and tested a piezoelectric vibration energy harvester integrated into landing struts of a 100 g quadrotor, generating electrical energy from rotor induced structural vibrations. A lead zirconate titanate (PZT) bimorph cantilever tuned to the rotor fundamental frequency (175 Hz at hover) demonstrated output power of 14.8 mW at resonance, which would extend hover time by 3.1% at typical nano UAV power levels. The harvester added only 2.3 g to system mass, and arrays of four harvesters were proposed to achieve 59 mW combined output and 12.4% endurance extension. Integration of such harvesters in nano drone landing gear provides a marginal but effectively mass efficient energy contribution requiring no additional active components.

Boyle et al. (2014) evaluated inductive wireless charging (Qi standard, 7.5 W at 100–200 mm coil separation) for automating nano drone battery recharging between deterrence patrols. A 35 mm diameter receive coil (3.8 g) compatible with 30 g nano quadrotors demonstrated charging of a 200 mAh LiPo cell to 80% capacity in 14 minutes via wireless transfer at 62% end to end efficiency. An autonomous drone docking pad prototype incorporating a Qi transmitter enabled autonomous landing and recharging without human intervention, supporting the concept of a self sustaining drone deterrence station maintaining continuous field coverage through multiple flight charge flight cycles across the agricultural day.

Choudhary et al. (2017) reviewed advances in lithium-polymer (LiPo) and lithium ion battery technology for UAV applications, analysing energy density trends over 2000–2016 using commercial cell manufacturer data. Pouch cell LiPo batteries reached specific energy densities of 180–200 Wh kg^{-1} by 2016, compared to 120 Wh kg^{-1} in 2005, a 55–67% improvement. For nano quadrotors at 30 g AUW with a 200 mAh, 3.7 V LiPo cell (4.5 g mass), achievable hover time at 2 W motor draw was calculated at 8.9 minutes consistent with observed 7–9 minute flight times for CX-10 class nano drones. Solid state electrolyte LiPo cells with projected energy density >300 Wh kg^{-1} were forecast for 2022–2025, potentially extending nano drone endurance to 12–15 minutes at equivalent cell mass.

Boukoberine et al. (2019) critically reviewed power supply systems for UAVs, comparing LiPo, hydrogen fuel cells, and solar panels. Proton exchange membrane fuel cell (PEMFC) systems achieved specific energy of 800–1,200 Wh kg^{-1} including hydrogen cylinder, providing 3–5× the energy density of LiPo batteries. However, minimum viable PEMFC system mass of 150–350 g made PEMFC impractical for nano drones below 50 g AUW. Solar PV integration on MAVs was evaluated as capable of providing 0.5–1.5 W supplemental power from 20 cm^2 of 22% efficiency monocrystalline cells, sufficient to extend nano drone hover time by 15–40% in full sunlight conditions suggesting solar assisted designs as a viable near term endurance extension strategy for daytime agricultural deterrence operations.

Wang et al. (2020) evaluated thermal management challenges of LiPo batteries in nano UAVs across 10°C to 45°C ambient conditions, measuring discharge capacity retention using an Arbin BT2000 battery analyser at 1C discharge rate. At 10°C, battery capacity fell to 54% of the rated 25°C value, reducing nano drone hover time from 8.2 to 4.4 minutes a critical constraint for bird deterrent deployment in temperate winter agricultural scenarios. A 0.8 g, 0.5 W heating film addition to the cell restored 91% of room-temperature capacity at 10°C, providing a practical cold weather operational solution for year-round deployment of the proposed system in temperate zones.

2.9 BIRD DETECTION MODELS

Cover and Hart (1967) proposed the K-Nearest Neighbour (KNN) algorithm as a simple yet effective supervised machine learning technique for pattern classification. The algorithm classifies an unknown sample based on the majority class of its nearest neighbours in the feature space. Owing to its non parametric nature and ease of implementation, KNN has been widely adopted in image processing, object recognition, and pattern classification tasks. Its ability to learn directly from training data without requiring complex model construction makes it suitable for real time applications with limited computational resources.

Stauffer and Grimson (1999) introduced the Adaptive Gaussian Mixture Model (GMM) as a robust background subtraction technique for real time object detection in video surveillance systems. The method models each pixel as a mixture of Gaussian distributions and continuously updates the background representation to accommodate gradual changes in illumination, shadows, and environmental conditions. Moving objects are identified as foreground regions when their pixel values deviate significantly from the learned background model. Due to its adaptability and computational efficiency, GMM has become one of the most widely used techniques for motion detection in outdoor environments.

Singh et al. (2018) applied GMM-based motion detection in agricultural monitoring systems for identifying moving pests and birds in crop fields. The study reported that GMM successfully extracted foreground objects from field video sequences and reduced the processing load by focusing subsequent analysis only on detected motion regions. The authors concluded that GMM provides an efficient first stage detection mechanism for smart farming applications and can be integrated with additional classification algorithms to improve object recognition accuracy. These findings support the use of GMM in the proposed bird detection and deterrent system for identifying bird activity in rice fields.

CHAPTER III

MATERIALS AND METHODS

This chapter deals with the materials used and methodology adopted to full fill the objectives of the study. It includes the details of the development of vision based bird deterrent system, ESP32 cam programming and various methods adopted for bird detection.

3.1 STUDY AREA

The experimental site was located at a geographical coordinate of latitude and longitude. The field study was conducted in the field of about 10 cents situated near the farm office at Kelappaji College of Agricultural Engineering and Food Technology (KCAEFT), Tavanur, Kerala.

3.2 TRADITIONAL METHODS OF BIRD REPELLENT SYSTEM

Traditional bird repellent methods have been widely employed in agricultural fields to protect crops from bird damage. Farmers commonly use scarecrows, reflective tapes, coloured flags, and predator models to deter birds from entering crop fields. These methods are simple, inexpensive, and easy to implement, making them popular among farmers, particularly in paddy growing regions. Manual guarding is also practiced, where farmers actively monitor fields and chase away birds during critical crop stages.

Physical barriers and sound based deterrents are other conventional techniques used in bird management. Bird nets are installed over crops to prevent birds from feeding, while noise making devices such as drums, crackers, and gas cannons are used to scare birds through sudden sounds. Although these methods can be effective to some extent, they often require considerable labour, maintenance, and operational costs. Moreover, large scale deployment of nets and continuous human supervision may not be feasible for extensive agricultural fields.

Despite their widespread use, traditional bird repellent methods have several limitations. Birds gradually become habituated to stationary deterrents such as scarecrows and reflective materials, reducing their effectiveness over time. Noise producing devices may cause disturbance to nearby

 

Plate 3.1 Conventional method

residents and livestock, while manual guarding is labour intensive and time consuming. These limitations highlight the need for automated and intelligent bird deterrent systems that can provide real time detection and efficient crop protection with minimal human intervention.

DEVELOPMENT OF BIRD DETECTION STATION WITH A DRON BASED DETERRENT SYSTEM

The bird detection and drone based deterrent system consists of two main units, a ground station and a drone mounted receiver station. The ground station uses an ESP32-CAM to continuously monitor the agricultural field, where the Gaussian Mixture Model (GMM) detects bird movement in real time. When a bird is detected, the system immediately sends a notification to the farmer and simultaneously transmits a wireless signal through a 433 MHz RF transmitter. The drone is manually operated by the user and carries the receiver unit, which consists of an RF receiver, Arduino Nano, and piezoelectric buzzer. Upon receiving the RF signal, the Arduino Nano activates the buzzer mounted on the drone, producing sound to scare birds away from the crop field. Thus, the system combines real time bird detection, instant farmer notification, wireless communication, and manual drone based bird deterrence using integrated hardware and software components. The following sections describe each component used in the development of the system.

3.3 DEVELOPMENT OF GROUND STATION

3.3.1 ESP32 Cam module and MB board

The ESP32-CAM equipped with the OV3660 camera sensor was used as the primary sensing and monitoring unit in the bird deterrent system. The module combines an ESP32 microcontroller with a high resolution camera, enabling image capture, wireless communication, and real time field monitoring. Due to its compact size, low power consumption, and integrated Wi-Fi capabilities, the ESP32-CAM is widely employed in smart agriculture and Internet of Things (IoT) applications. In our study, the ESP32-CAM was installed in the paddy field for continuous surveillance of bird activity. The camera continuously monitored the field and detected movement within its field of view. Upon detection of motion, the microcontroller generated an output signal to activate the deterrent mechanism, thereby helping to reduce bird damage in crops. The ESP32-CAM module was programmed using the Arduino IDE software. The firmware was uploaded through the ESP32-CAM-MB programmer. The system operated on a regulated 5 V DC power supply to ensure stable performance under field conditions.

The OV3660 camera sensor provides improved image quality and supports high resolution image capture, making it suitable for agricultural monitoring applications. The wireless communication capability of the ESP32-CAM allows future integration with cloud based monitoring and remote control systems. Thus, the ESP32-CAM with OV3660 camera sensor served as an efficient and cost effective platform for developing an automated bird monitoring and deterrent. The ESP32-CAM is a small, low cost development board based on the ESP32 microcontroller and a camera module. It combines Wi-Fi and Bluetooth connectivity with a camera, making it suitable for projects requiring image capture and wireless communication capabilities. The ESP32-CAM was mounted at an appropriate height in the field to monitor crop areas susceptible to bird attack. The module continuously captured images and performed motion based detection to identify the presence of birds. When movement was detected, the controller activated the deterrent system to scare away birds from the crop field. This automated monitoring system minimized the need for manual surveillance and improved crop protection efficiency. The specifications of ESP32-CAM is given in the following table 3.1.

3.3.1.1 Camera Module

The ESP32-CAM integrates a small camera module, typically an OV3660, capable of capturing images and video. The camera can be used to capture still images or stream video to a host device. The OV3660 sensor supports up to 2048 × 1536 (3 MP) image capture.

3.3.1.2 GPIO Pins

The ESP32-CAM features a set of general-purpose input/output (GPIO) pins that allow you to connect additional sensors, actuators, or other components to expand the functionality of your project.

3.3.1.3 Storage Options

The board offers different storage options for storing images and other data. It includes a microSD card slot for external storage, as well as built-in flash memory for storing firmware and other files.

3.3.1.4 Programming

The ESP32-CAM can be programmed using the Arduino IDE, which provides a user friendly development environment for writing and uploading code. There are also alternative programming options available, such as MicroPython or the Espressif IDF (IoT Development Framework).For programme uploading esp32 cam connect along with its esp 32 cam mb board.

3.3.1.5.Power Supply

The board can be powered through a USB connection or an external power source. It has a voltage regulator to provide a stable power supply to the ESP32 and camera module.

The ESP32-CAM is commonly used in applications such as surveillance systems, home automation, robotics, and IoT projects that require image capture and wireless connectivity. Its compact size and affordable price make it a popular choice for hobbyists and developers.

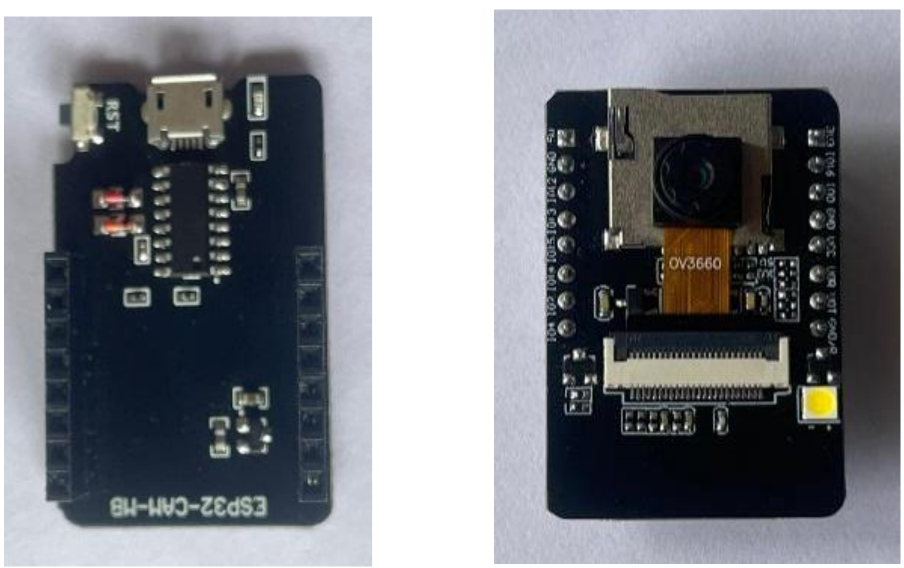

Plate 3.2 ESP32 CAM MB board and ESP32 CAM

Table 3.1 Specifications of Microcontroller

SL NO.	PARAMETERS	SPECIFICATIONS
1	Microcontroller	ESP32 Dual-Core Xtensa LX6
2	CPU Frequency	240 MHz
3	Flash Memory	4 MB
4	PSRAM	4 MB
5	Camera Sensor	OV3660
6	Camera Resolution	3 MP (2048 × 1536 pixels)
7	Input Voltage	5 V input
8	Operating Voltage	3.3 V
9	Storage	MicroSD card support
10	Power Consumption	80–300 mA

3.3.2 RF Transmitter module

The 433 MHz RF transmitter module was selected for the present study due to its low cost, low power consumption, and ease of interfacing with microcontrollers such as the ESP32-CAM. The module provides reliable wireless communication over moderate distances, making it suitable for agricultural field applications where wired connections are impractical. Its compact size and lightweight design facilitate easy integration with the ground station without adding significant complexity to the system. Furthermore, the RF transmitter enables real time transmission of bird detection signals from the ground station to the drone mounted receiver. The use of wireless communication enhances system flexibility and allows remote activation of the deterrent mechanism only when bird activity is detected, thereby improving energy efficiency. Owing to these advantages, the 433 MHz RF transmitter was chosen as the communication module for the developed bird deterrent system.

A 433 MHz Radio Frequency (RF) transmitter module was employed in the ground station of the bird deterrent system to facilitate wireless communication between the sensing unit and the drone mounted deterrent unit. The transmitter was interfaced with the ESP32-CAM module, which acted as the central processing and monitoring unit of the system. The ground station was strategically positioned to monitor bird activity in the crop field. The ESP32-CAM continuously captured images of the field and performed bird detection. Upon detection of bird movement, the ESP32-

CAM generated a digital output signal, which was supplied to the RF transmitter module for wireless transmission.

The RF transmitter operates at a carrier frequency of 433 MHz using Amplitude Shift Keying (ASK) modulation. In this modulation technique, digital information is transmitted by varying the amplitude of the carrier wave. The transmitter converts the electrical signals received from the ESP32-CAM into radio frequency waves and radiates them through an antenna to the receiver mounted on the drone. The use of RF communication enables long range signal transmission without the need for physical wiring, thereby improving system flexibility and ease of deployment under field conditions. The wireless link allows the drone to receive control signals in real time and activate the deterrent mechanism only when bird is detected, thereby reducing unnecessary operation and conserving power. The transmitter module operates at a supply voltage ranging from 3 V to 12 V DC and exhibits low power consumption, making it suitable for portable and battery operated agricultural applications. The module is compact, lightweight, inexpensive, and easy to interface with microcontrollers, making it effective. In our study, the RF transmitter served as the communication bridge between the ground-based monitoring unit and the aerial deterrent unit, ensuring timely transmission of detection signals for effective bird management in paddy cultivation. The specifications of transmitter is mentioned in the table 3.2.

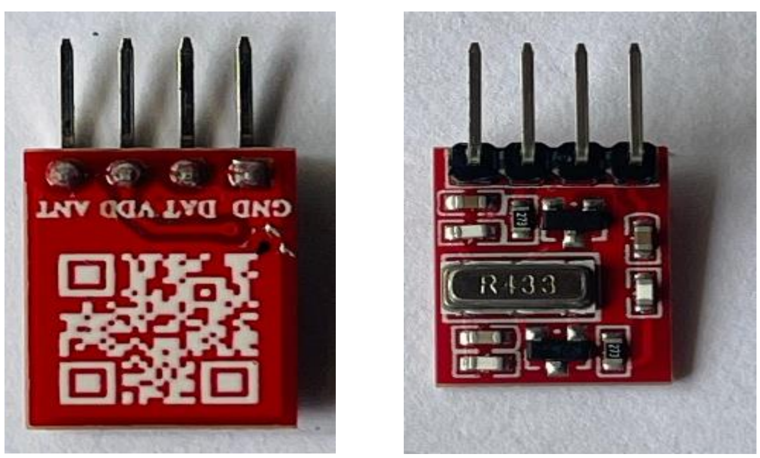

Plate 3.3 433 MHz transmitter

Table 3.2 Specifications of Transmitter

SL NO.	PARAMETER	SPECIFICATION
1	Operating Frequency	433 MHz
2	Operating Voltage	3–12 V
3	Modulation Technique	ASK (Amplitude Shift Keying)
4	Transmission Range	50–100 m in open field conditions
5	Power Consumption	Low
6	Communication Type	Wireless RF communication

3.3.3 AC Power Supply for Ground Station

An AC power supply was utilized to provide a stable and continuous source of electrical power to the ground station of the bird deterrent system. The ground station consisted of the ESP32-CAM module, RF transmitter module, and other associated electronic components responsible for bird detection and signal transmission. Since these components require a regulated DC voltage for proper operation, the available AC mains supply was converted into a suitable DC output using an AC to DC adapter.

The selection of an AC power supply was based on its reliability, availability, and ability to provide a constant power output for long duration operation. Compared to battery powered systems, the AC power supply offers greater operational stability and reduces maintenance requirements. Therefore, it was adopted as the primary power source for the ground station to ensure efficient functioning of the bird detection and wireless communication system throughout the experimental period.

The AC power supply ensured uninterrupted operation of the ground station during field monitoring. A regulated 5 V DC output was provided to the ESP32-CAM and RF transmitter module, maintaining stable performance and preventing voltage fluctuations that could affect system reliability. The use of an AC power source eliminated the need for frequent battery replacement or recharging, thereby enabling continuous monitoring of bird activity over extended periods.

3.4 DEVELOPMENT OF RECEIVER SIDE

3.4.1 Drone

A drone (Model: LLCDRR01) was utilized as the aerial platform for the bird deterrent system. The drone served as the carrier for the RF receiver, Arduino Nano, and buzzer assembly. Upon receiving a bird detection signal from the ground station, the onboard electronics activated the deterrent mechanism mounted on the drone. The compact design, stable flight characteristics, and ease of operation made the drone suitable for experimental evaluation of the proposed bird deterrent system. The drone was capable of remote operation and provided sufficient payload capacity to accommodate the lightweight electronic components used in the study.

The drone was selected due to its lightweight construction, ease of operation, and adequate flight duration and affordability. Features such as altitude hold and stable flight control enabled smooth operation during testing, while the compact structure allowed integration of additional electronic components without significantly affecting flight performance. The drone also provided sufficient communication range and maneuverability for small-scale agricultural field applications. Furthermore, its low cost compared with professional UAV platforms made it a practical choice for development and experimental research in agriculture. The selected drone incorporates features such as altitude hold, headless mode, return home function, and stable wireless control as shown in fig 3.1. It is powered by rechargeable lithium polymer batteries and offers a maximum operating range of approximately 150 feet. The drone also includes dual cameras and Wi-Fi connectivity. The drone functioned primarily as an aerial deterrent platform capable of carrying and operating the RF based warning system. The specifications of the nano toy drone is given in table 3.3.

Fig.3.1 Diagram of Nano drone

 

Plate 3.4 Nano drone

Table 3.3 Specifications of Nano Drone

SL NO.	PARAMETER	SPECIFICATION
1	Model	LLCDRR01
2	Battery type	2 batteries of Lithium Polymer (Li-Po)
3	Battery capacity	2 × 1300 mAh
4	Flight time	Up to 30 min (combined)
5	Control method	Remote Control and Mobile App (Nabhyan)
6	Communication	Wi-Fi
7	Camera	Dual Camera (1080P and 720P)
8	Maximum range	Approximately 150 ft

3.4.2 DC Power Supply for Receiver Station

A DC power supply using a coin cell battery as shown in plate 3.5, was utilized to provide power to the receiver station of the bird deterrent system. The receiver station consisted of the Arduino Nano, RF receiver module, and buzzer, responsible for receiving the transmitted signal and activating the deterrent mechanism. Since these components operate at low current and voltage levels, a compact coin battery was sufficient to meet their power requirements without the need for an external power adapter.

The selection of a coin battery as the power source was based on its compact size, portability, and suitability for low power, intermittent operation. Unlike the ground station, which required continuous power for sensing and transmission, the receiver station operated in short bursts only when triggered, making a battery based supply a practical and energy efficient choice. This also allowed the receiver unit to be placed independently in the field without dependence on a fixed AC outlet.

The coin battery ensured reliable operation of the receiver station during field deployment. A stable DC output was supplied to the Arduino Nano, RF receiver module, and buzzer, enabling prompt activation of the deterrent sound upon receiving the transmitted signal. The use of a battery powered receiver allowed for flexible placement at the deterrence site, while its low power consumption ensured the battery lasted throughout the experimental period without frequent replacement.

Plate 3.5 CR2032 cell battery

3.4.3 Arduino Nano

An Arduino Nano microcontroller board as shown in plate 3.6, was employed on the drone as the primary control unit for processing the wireless signals received from the ground station. The board is based on the ATmega328P microcontroller and offers a compact, lightweight, and low power solution suitable for drone based applications. Due to its small form factor and ease of interfacing with various electronic components, the Arduino Nano was selected for integration with the RF receiver and deterrent mechanism mounted on the drone.

The Arduino Nano was selected for the drone unit due to its compact dimensions, lightweight design, and ease of programming. Unlike larger microcontroller boards, the Nano occupies minimal space and adds negligible weight to the drone, which is an important consideration for maintaining flight efficiency and stability. The board also provides sufficient processing capability for handling RF communication and controlling the deterrent mechanism. Furthermore, the Arduino Nano offers compatibility with a wide range of communication modules and peripherals, enabling seamless integration with the RF receiver used in the present study. Its low cost, reliable performance, and extensive community support make it an ideal choice for development and agricultural automation applications.

In the developed bird deterrent system, the Arduino Nano was connected to the 433 MHz RF receiver module. The receiver continuously monitored incoming signals transmitted from the ESP32-CAM based ground station. Upon receiving a valid bird detection signal, the Arduino Nano processed the received data and activated the deterrent mechanism mounted on the drone. This enabled rapid response to bird intrusion while minimizing unnecessary operation of the deterrent system.

The Arduino Nano operates at a frequency of 16 MHz and provides multiple digital and analog input/output pins for interfacing with sensors, communication modules, and actuators. The board was powered using the drone power supply and exhibited stable performance throughout the experimental period. The specifications of the nano toy drone is given in table 3.4.

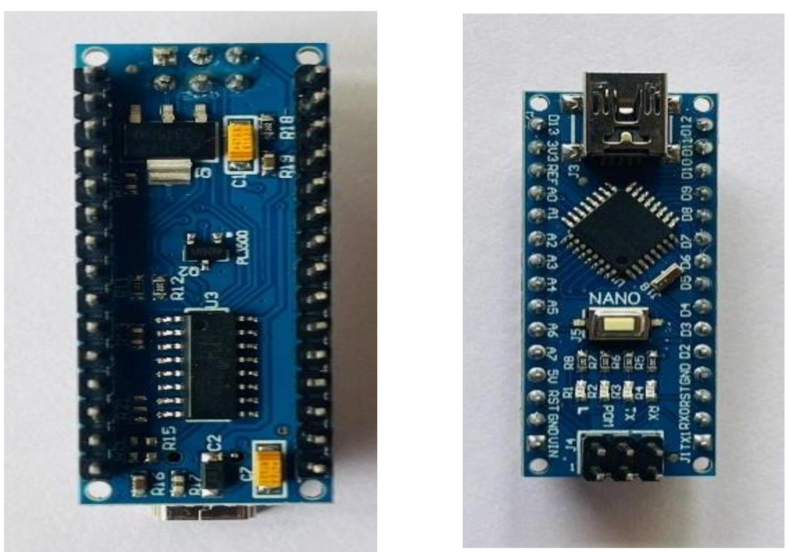

Plate 3.6 Arduino Nano

Table 3.4 Specifications of Arduino nano

SL NO.	PARAMETER	SPECIFICATION
1	Microcontroller	ATmega328P
2	Operating Voltage	5 V
3	Input voltage	7-12 V
4	Frequency	16MHz
5	Digital I/O pin	14
6	Analog input pin	8
7	PMW pin	6
8	Flash memory	32 KB
9	SRAM	2 KB

3.4.4 RF Receiver Module

A 433 MHz Radio Frequency (RF) receiver module as shown in plate 3.7, was employed in the drone unit of the bird deterrent system to receive wireless signals transmitted from the ground station. The receiver served as the communication interface between the ESP32-CAM based monitoring unit and the drone mounted deterrent mechanism.

The 433 MHz RF receiver module was selected for our project owing to its compatibility with the RF transmitter module, low power consumption, and reliable signal reception under field conditions. The module offers adequate communication range for agricultural applications and can operate efficiently without internet connectivity. The compact and lightweight design of the receiver makes it highly suitable for drone integration, as it imposes minimal additional load on the aerial platform. Furthermore, the receiver can be easily interfaced with microcontrollers and other electronic components, thereby simplifying system development and implementation.

The receiver module was mounted on the drone and continuously monitored for incoming radio frequency signals transmitted by the RF transmitter located at the ground station. Whenever bird activity was detected in the crop field, the ESP32-CAM generated a control signal, which was wirelessly transmitted through the RF transmitter. The RF receiver captured the transmitted signal and converted it into an electrical output that could be processed by the control circuitry on the drone.

The receiver operates at a carrier frequency of 433 MHz and is designed to receive signals modulated using Amplitude Shift Keying (ASK) technique. The received signal is demodulated and delivered as digital data to the connected controller or actuation system. Upon reception of the signal, the deterrent mechanism mounted on the drone was activated to scare away birds from the crop field.

The use of a wireless receiver on the drone eliminated the requirement for wired communication and enabled efficient operation over large agricultural areas. The receiver exhibited reliable signal reception under open field conditions and ensured timely activation of the deterrent system. Its compact size and lightweight construction made it suitable for integration with drone platforms without significantly affecting payload or flight performance.

The RF receiver operates at a regulated supply voltage of 5 V DC and consumes very low power, thereby extending the operational duration of battery powered systems. Due to its simple interfacing and dependable performance, the module was effectively integrated into the developed bird deterrent system.

In the our study, the RF receiver acted as the endpoint of the wireless communication network, receiving bird detection signals from the ground station and initiating the corresponding response on the drone for effective bird management in paddy cultivation. The specifications of the nano toy drone is given in table 3.5.

Plate 3.7 433 MHz receiver

Table 3. 5 Specifications of receiver

SL NO.	PARAMETER	SPECIFICATION
1	Operating Frequency	433 MHz
2	Operating Voltage	5V
3	Modulation Technique	ASK (Amplitude Shift Keying)
4	Transmission Range	50–100 m in open field conditions
5	Power Consumption	Low
6	Communication Type	Wireless RF communication

3.4.5 Piezoelectric Buzzer

A piezoelectric buzzer as shown in plate 3.8, was used as the deterrent device in the drone unit of the bird deterrent system. The buzzer is an electronic sound producing component that converts electrical energy into audible sound waves. It is widely used in alarm systems, warning devices, and embedded electronic applications due to its simple construction, low power consumption, and reliable operation.

The buzzer was selected for this study because of its lightweight design, compact size, low power requirement, and ease of interfacing with microcontrollers. These characteristics make it suitable for drone based applications where payload weight and power consumption must be minimized. Furthermore, the buzzer provides an immediate audible response upon activation, enabling rapid bird deterrence without the need for complex mechanical systems.In our project, the buzzer was interfaced with the Arduino Nano mounted on the drone. The Arduino Nano continuously monitored signals received from the RF receiver module. When a bird detection signal was transmitted from the ESP32-CAM based ground station and received by the drone, the Arduino Nano activated the buzzer. The generated sound acted as an acoustic deterrent to scare birds away from the crop field, thereby helping to reduce crop damage. The specifications of piezoelectric buzzer is mentioned in table 3.6.

Plate 3.8 Piezoelectric Buzzer

Table 3.6 Specifications of buzzer

SL NO.	PARAMETER	SPECIFICATION
1	Operating Voltage	3–5V
2	Operating mode	Continuous
3	Power Consumption	Low

3.5 ARDUINO IDE SOFTWARE

Arduino Integrated Development Environment (Arduino IDE) was used as the programming platform for developing and uploading the firmware required for the bird deterrent system. Arduino IDE is an open source software application as shown in plate3.9, that provides a user-friendly environment for writing, compiling, debugging, and uploading programs to microcontroller boards. It supports a wide range of development boards.

In this project, Arduino IDE was utilized to develop the control algorithms for image acquisition, bird detection, wireless communication, and activation of the deterrent mechanism. The software enabled the programming of the ESP32-CAM for field monitoring and the Arduino Nano for processing signals received through the RF receiver. The generated source code was compiled and uploaded to the respective microcontrollers through USB-based programming interfaces.

Arduino IDE was selected because of its simplicity, extensive library support, and compatibility with various hardware platforms. The software provides numerous built in and third party libraries for camera modules, wireless communication, sensors, and IoT applications, which significantly reduced development time. Furthermore, its open source nature, active user community, and cross platform compatibility make it one of the most widely used software tools for embedded system and agricultural automation projects.

3.5.1 Features of Arduino IDE

- Open source and freely available software.
- Supports multiple microcontroller platforms.
- Provides an integrated code editor, compiler, and serial monitor.
- Compatible with ESP32-CAM and Arduino Nano boards.
- Supports a wide range of libraries for sensors and communication modules.
- Facilitates easy code uploading and debugging.
- Available for Windows, Linux, and macOS operating systems.

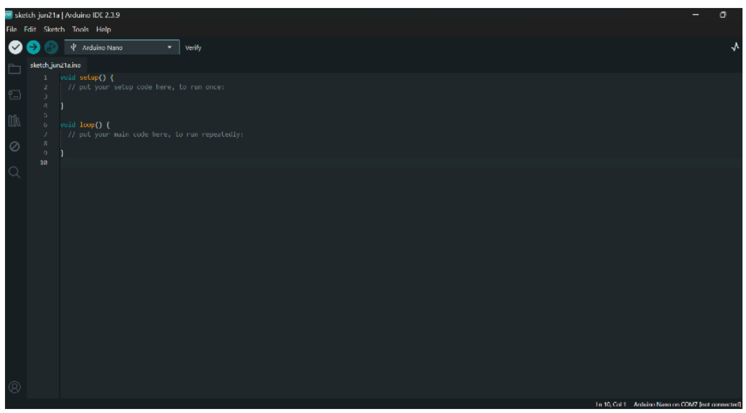

Plate 3.9 Arduino IDE software interface

3.5.2 Steps to Upload Code

- Connect the Arduino or compatible board via USB
- Select the board from Tools > Board
- Select the correct COM port from Tools > Port
- Click the Upload button (right arrow icon)

The IDE will compile the code, convert it to machine instructions, and upload it to the microcontroller's flash memory.

3.5.2.1 Setting Up of Arduino IDE

- Install & create account in Arduino IDE
- Connect the ESP32 CAM board Using USB cable
- Open the Arduino IDE

- Select Board and Port
- Write or open a sketch
- Upload the sketch
- Check the output data
- Creating an Arduino account

3.5.2.2 Connect the ESP32 CAM module

Connect the ESP32 CAM module to the computer using a USB cable to power it and enable communication for uploading code.

Plate 3.10 Connection of ESP32 CAM module

3.5.2.3 Open the Arduino IDE

Open the Arduino IDE on your computer to write, compile, and upload code to the ESP32 CAM. Prior to uploading, the required board packages and libraries were installed in the Arduino IDE. For this “esp32 espressif” package and “universal telegram bot” libraries were installed.

3.5.2.4 Select Board and Port

In the Arduino IDE, go to the "Tools" menu, select the “AI THINKER ESP 32”, and then choose the correct COM port 6 to establish communication with the connected ESP 32 CAM.

3.5.2.5 Write or open a sketch

Write a new sketch for camera initialistaion in the Arduino IDE ,later write code for message notification when image frame difference occurred within 1000 as threshold and sending rf signal to receiver to define the instructions that will be uploaded and executed on the ESP32 CAM. The code used is mentioned in Appendix I.

3.5.2.6 Upload the sketch

Click the Upload button in the Arduino IDE to compile the sketch and transfer it to the ESP32 CAM. Once uploaded, the board will automatically start running the program.

3.5.2.7 Check the output data

Open the Serial Monitor from the Tools menu in the Arduino IDE and set the baud rate as 115200 to view and verify the output data being sent from the ESP32 CAM as in plate 3.11.

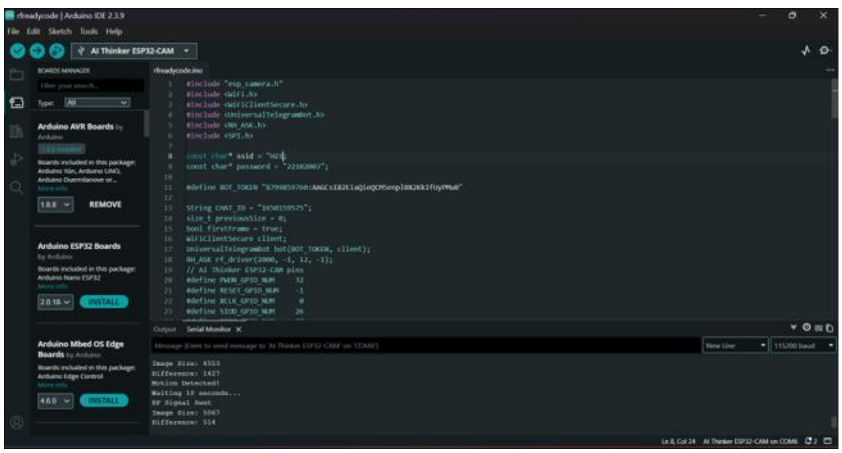

Plate 3.11 Serial monitoring of esp32 cam

3.5.2.8 Connect the ARDUINO NANO module

Connect the ARDUINO NANO module to the computer using a USB cable to power it and enable communication for uploading code.

3.5.2.9 Open the Arduino IDE

Open the Arduino IDE on your computer to write, compile, and upload code to the ARDUINO NANO. Prior to uploading, the required board packages and libraries were installed in the Arduino IDE. For this “Arduino AVR boards” package was installed.

3.5.2.10 Select Board and Port

In the Arduino IDE, go to the "Tools" menu, select the “ARDUINO NANO”, and then choose the correct COM port 6 to establish communication with the connected Arduino board.

3.5.2.11 Write or open a sketch

Write a new sketch for recieveing the sended rf signal and to activate the buzzer for specified time to define the instructions that will be uploaded and executed on the ARDUINO NANO.

3.5.2.12 Upload the sketch

Click the Upload button in the Arduino IDE to compile the sketch and transfer it to the ARDUINO NANO. Once uploaded, the board will automatically start running the program after receiving the signal.

3.5.2.13 Check the output data

Open the Serial Monitor from the Tools menu in the Arduino IDE and set the baud rate as 115200 to view and verify the output from the Arduino Nano.

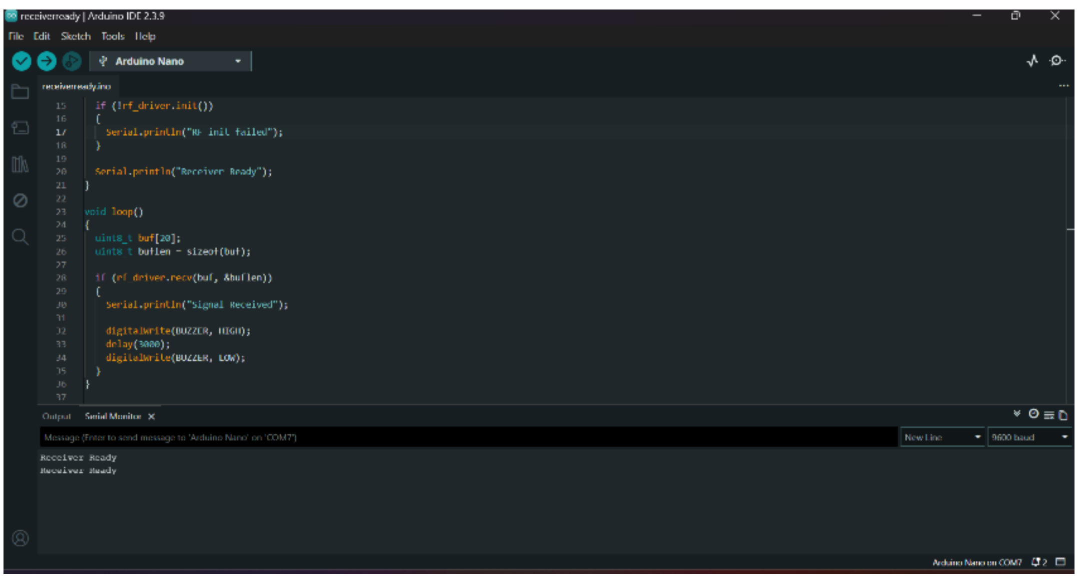

Plate 3.12 Serial monitoring of arduino nano

3.6 CIRCUIT CONNECTION

The circuit diagram was created using Cirkit Designer IDE website.The circuit diagram with all the hardware components are shown below in fig.3.2 & 3.3 and plate 3.13 &3.14. Connections are made accordingly and finally checked with the code.

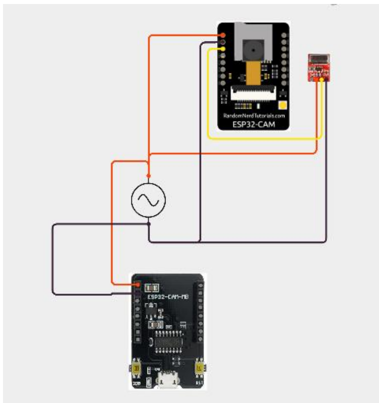

Fig 3.2 Circuit diagram of ground station

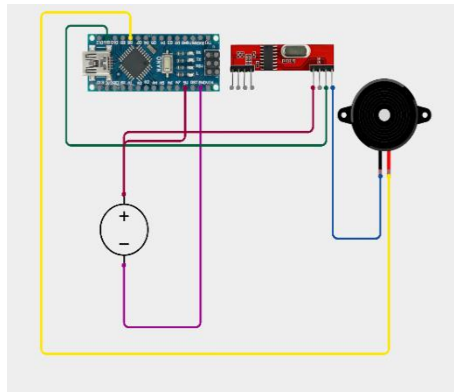

Fig 3.3 Circuit diagram of receiver side

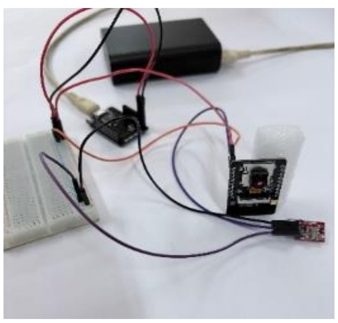

Plate 3.13 Ground component connection

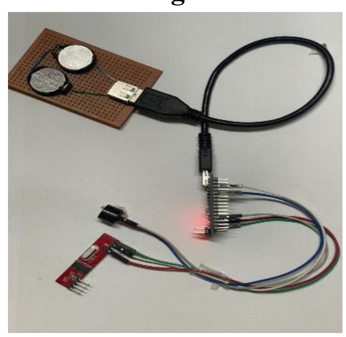

Plate 3.14 Receiver connection

3.7 BIRD DETECTION MODELS

3.7.1 Gaussian Mixture Model (GMM)

The Gaussian Mixture Model (GMM) is a probabilistic statistical method widely used for background modeling and foreground object detection in video surveillance and computer vision applications. The model was introduced by Stauffer and Grimson (1999) and has become one of the most effective techniques for detecting moving objects in dynamic environments. In GMM, each pixel in a video sequence is represented by a mixture of several Gaussian distributions rather than a single distribution. This enables the model to adapt to variations in illumination, repetitive background motion, shadows, and other environmental changes.

The fundamental concept of GMM is based on the assumption that the intensity values of a pixel over time can be represented as a combination of K Gaussian distributions. Each Gaussian component is characterized by three parameters: mean (μ), variance (σ^2), and weight (ω). The mean represents the average pixel value, the variance indicates the spread of the pixel values around the mean, and the weight represents the probability of occurrence of that Gaussian component .Unlike hard clustering methods, which assign each data point to only one cluster, GMM performs soft clustering by assigning probabilities. For example, a data point may have an 80% probability of In the proposed bird detection and deterrent system, the Gaussian Mixture Model is employed to identify motion within the field of view captured by the ESP32-CAM. By continuously updating the background model, the algorithm effectively distinguishes moving birds from the static background, enabling accurate detection under varying environmental conditions. The detected foreground regions are then used to trigger the deterrent mechanism, thereby reducing crop damage caused by bird intrusion.

The major advantages of GMM include adaptability to changing environmental conditions, robustness against illumination variations, capability to model dynamic backgrounds, and suitability for real time applications. However, the method requires careful selection of parameters such as the number of Gaussian components, learning rate, and threshold values to achieve optimal detection performance. Despite these limitations, GMM remains one of the most widely adopted techniques for motion detection and background subtraction in intelligent surveillance and agricultural monitoring systems.

3.7.2 K-Nearest Neighbors (KNN)

The K-Nearest Neighbors (KNN) algorithm is a non parametric machine learning method used for classification and pattern recognition. In background subtraction, KNN classifies each pixel as either background or foreground by comparing its current value with a history of previously observed pixel values. Unlike Gaussian Mixture Models, KNN does not assume any predefined probability distribution. Instead, it stores a set of recent pixel samples and determines whether the current pixel belongs to the background based on the number of neighboring samples within a specified distance threshold.

For each incoming pixel value, the Euclidean distance between the current sample and stored background samples is calculated. If at least K neighboring samples are found within the threshold distance, the pixel is classified as background; otherwise, it is considered part of a foreground object. The background model is continuously updated by replacing old samples with new observations, enabling the algorithm to adapt to gradual scene changes.

KNN offers several advantages, including simplicity, robustness to dynamic backgrounds, and the ability to handle multimodal pixel distributions without requiring complex parameter estimation. Due to its adaptive nature and computational efficiency, KNN is widely used in real time surveillance, object tracking, motion detection, and agricultural monitoring applications. In the proposed bird deterrent system, the KNN algorithm can be employed to detect moving birds by distinguishing foreground motion from the static background captured by the camera, thereby enabling timely activation of the deterrent mechanism.

The captured images were first preprocessed and labeled according to ground truth (bird present or absent) to form a structured dataset suitable for supervised evaluation. In the GMM-based approach, each pixel's intensity distribution across the sample frames was modeled as a mixture of Gaussian components, allowing background and foreground (bird) pixels to be statistically separated based on their probability of belonging to the learned background distribution; the resulting foreground pixel counts across the labeled dataset were then analyzed to identify the threshold value that best discriminated bird-present frames from background only frames. In parallel, a KNN classifier was applied directly to extracted frame features (changed pixel count and related descriptors) to classify each sample as bird-present or background, using a range of candidate threshold/distance values to determine the configuration yielding the highest classification accuracy. The detection outputs of both models were systematically compared across the labeled dataset to evaluate their respective accuracy, false positive rate, and false negative rate at varying threshold settings. Through this comparative optimization process, GMM is identified as the best method for detection of birds and the threshold value that consistently produced the most accurate and reliable separation between bird and non bird frames across both modeling approaches was identified and selected as the optimum operating threshold. This optimized threshold was subsequently fixed and embedded into the ESP32-CAM detection code.

3.8 METHODOLOGY

The proposed system consists of two major units: a ground station and a drone mounted deterrent unit. The ground station comprises an ESP32-CAM module, ESP32-CAM-MB programmer, RF transmitter, and AC power supply. The drone unit consists of an RF receiver, Arduino Nano microcontroller, and buzzer. The overall methodology involves image acquisition, bird detection, wireless signal transmission, and activation of a deterrent mechanism.

Initially, the ground station is powered using a regulated AC power supply. Upon startup, the ESP32-CAM establishes a Wi-Fi connection and initializes all the required peripherals, including the camera module and RF transmitter. Once initialization is completed, the ESP32-CAM begins continuous monitoring of the agricultural field by capturing image frames at regular intervals of 3 seconds. The captured images are used for bird detection and monitoring purposes.

The bird detection process is carried out using the Gaussian Mixture Method (GMM) implemented. Images captured by the ESP32-CAM are processed using the GMM algorithm, which models image pixel distributions using multiple Gaussian functions. The method effectively separates objects of interest from the background and identifies the presence of birds within the captured image. The algorithm is capable of handling variations in illumination and environmental conditions, making it suitable for outdoor agricultural applications.

Whenever the Gaussian Mixture Method detects the presence of birds in the monitored area, the ESP32-CAM generates a detection event. Simultaneously, a notification message is transmitted through a Telegram bot to inform the user about bird activity in the field. This enables remote monitoring of the agricultural area and provides immediate information regarding bird intrusion.

Following bird detection, the system waits for a predefined interval about 10 seconds before initiating the buzzer action. The ESP32-CAM then sends a wireless command through the 433 MHz RF transmitter module. The RF transmitter converts the digital command generated by the ESP32-CAM into radio frequency signals and broadcasts them to the receiver unit mounted on the drone.

The transmitted RF signal is received by the 433 MHz RF receiver installed on the drone. The receiver continuously listens for incoming signals from the ground station and forwards the received data to the Arduino Nano microcontroller. The Arduino Nano acts as the central processing unit of the drone-mounted deterrent system and interprets the received command.

Upon successful reception of the bird detection signal, the Arduino Nano activates the buzzer connected to the output pin of the microcontroller. The buzzer generates an audible sound intended to scare birds away from the crop field. The sound acts as an acoustic deterrent, reducing the likelihood of birds feeding on the crops and thereby minimizing crop losses.


Plate 3.15 Drone field deployment

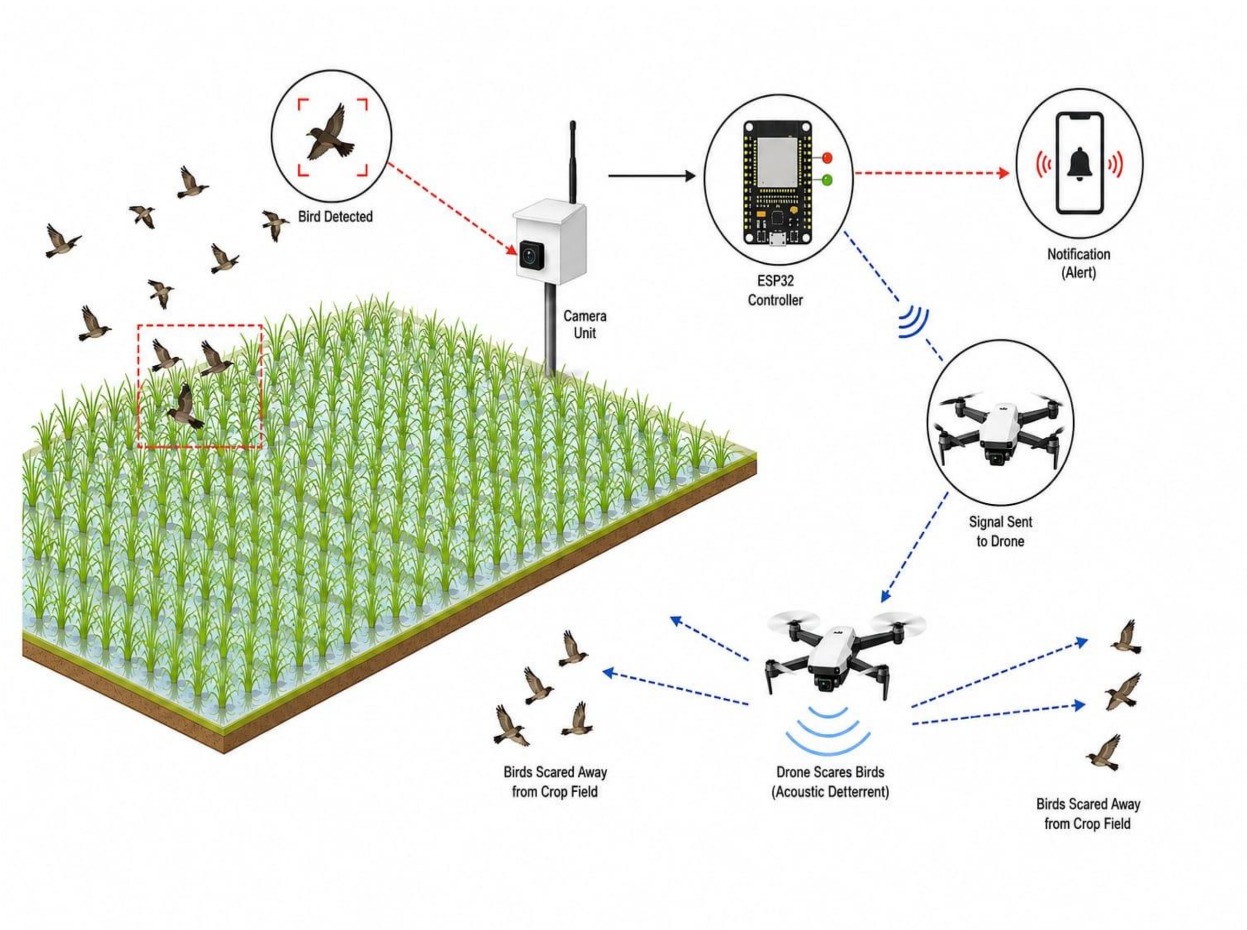

Fig 3.4 Diagrammatic representation of bird detection station with drone based deterrent system

3.9 COST ECONOMICS

The economic feasibility of the developed bird deterrent and detection drone system was evaluated on the basis of fixed cost, operating cost, cost of operation, annual benefit, benefit-cost ratio, break-even point, and payback period, computed using standard farm machinery costing procedures.

3.9.1 Fixed Cost

Depreciation

Depreciation was calculated using the straight-line method:

$$D = (P - S) / L$$

Interest

Interest on investment was calculated as:

$$I = ((P + S) / 2) \times i$$

Shelter, Taxes and Insurance

Cost towards shelter, taxes and insurance was estimated as:

$$STI = 0.02 \times P$$

The total fixed cost per hour was obtained as the sum of depreciation, interest, and shelter, taxes and insurance:

Fixed Cost = D + I + STI

3.9.2 Operating Cost

Electricity Cost

Electricity cost (battery charging) was calculated as:

$$\text{Electricity Cost} = \text{Charger Power (kW)} \times \text{Duty Cycle} \times \text{Tariff (₹/kWh)}$$

Labour Cost

Labour cost, applicable only if a dedicated operator is engaged, was calculated as:

$$\text{Labour Cost} = \text{Daily Wage} / \text{Working Hours per Day}$$

Repair and Maintenance

Repair and maintenance cost was estimated as:

$$R\&M = (0.06 \times P) / \text{Annual Working Hours}$$

The total operating cost per hour was obtained as:

$$Operating\ Cost = Electricity\ Cost + Labour\ Cost + R\&M$$

3.9.3 Total Cost of Operation

The total cost of operation per hour was calculated as:

$$TC = Fixed\ Cost/h + Operating\ Cost/h$$

3.9.4 Continuous Monitoring Cost

Unlike the drone, which flies only during the bird active periods, the ESP32-CAM module monitors the field continuously (24 h/day) for bird detection. Its energy cost was calculated separately as an annual overhead:

$$Monitoring\ Cost = Camera\ Power\ (kW) \times 24 \times 365 \times Tariff\ (₹/kWh)$$

3.9.5 Annual Value of Crop Protected

Annual paddy production in the protected area was estimated as:

$$Annual\ Production = Area\ Protected \times Yield\ per\ Acre \times Cropping\ Seasons/Year$$

The value of this production, and the annual benefit obtained by preventing bird damage, were calculated as:

$$Crop\ Value = Annual\ Production \times Price\ per\ kg$$

$$Annual\ Benefit = Crop\ Value \times Damage\ Rate\ (without\ deterrent) \times Deterrent\ Effectiveness$$

3.9.6 Annual Operating Expense

Annual operating expense was calculated as:

$$Annual\ Expense = (TC \times Annual\ Working\ Hours) + Monitoring\ Cost$$

3.9.7 Annual Net Benefit

Annual net benefit was calculated as:

$$Net\ Benefit = Annual\ Benefit - Annual\ Expense$$

3.9.8 Benefit-Cost Ratio

The benefit-cost ratio was calculated as:

$$B : C\ Ratio = Annual\ Benefit / Annual\ Expense$$

3.9.9 Break-even Point

Variable cost per acre-season was calculated as:

$$Variable\ Cost = (Operating\ Cost/h \times Annual\ Working\ Hours + Monitoring\ Cost) / (Area \times Seasons)$$

Contribution margin was calculated as:

$$Contribution = Benefit\ per\ Acre\text{-}season - Variable\ Cost$$

The break-even point was determined as:

$$BEP = Fixed\ Cost / Contribution$$

3.9.10 Payback Period

The payback period was calculated as:

$$Payback\ Period = Initial\ Investment / Annual\ Net\ Benefit$$

where, P = fabrication cost of the unit (₹), S = salvage value (₹), L = economic life (years), and i = rate of interest (decimal).

CHAPTER IV

RESULTS AND DISCUSSION

This chapter presents the results obtained from the development and evaluation of the proposed bird detection and drone based deterrent system. Initially, the performance of the Gaussian Mixture Model (GMM) and K-Nearest Neighbour (KNN) algorithms was analysed by comparing their True Positive Rate (TPR), False Positive Rate (FPR), and bird detection accuracy at different threshold values to identify the optimal detection model. Based on the evaluation, the GMM model demonstrated superior performance and was selected for implementation in the developed system. The effectiveness of the proposed system was then validated through field experiments by comparing its bird deterrence performance with the conventional manual bird scaring method using bird return time as the evaluation parameter.

4.1 MODEL OPTIMISATION AND PERFORMANCE ANALYSIS

The GMM and KNN background subtraction models were each tested across a range of thresholds, with detections at every threshold checked against the ground truth of 30 birds to compute the True Positive Rate (TPR) and False Positive Rate (FPR). The sections below present each model's results separately, then compare them to identify the best performing model and threshold.

4.1.1 Gaussian Mixture Model (GMM) Optimization

The GMM was evaluated across eleven candidate probability threshold values ranging from 0.3 to 0.99 as in fig 4.1 & 4.2 given below.

Fig 4.1 Optimisation of GMM at 0.3 threshold

Fig 4.2 Optimisation of GMM at 0.99 threshold

For each threshold, the total number of foreground detections flagged by the model, the number of those detections that correctly corresponded to an actual bird (true detected birds), and the resulting recall, specificity, and false positive rate were recorded. The complete dataset is presented in Table 4.1.

Table 4.1 GMM model detection performance across thresholds

Threshold	Actual No. of Birds	Detected No. of Birds	True Detected Birds	True Positive Rate	False Positive Rate
0.30	30	145	27	0.900	0.739
0.40	30	138	27	0.900	0.722
0.50	30	127	27	0.900	0.691
0.60	30	120	27	0.900	0.667
0.70	30	114	27	0.900	0.643
0.80	30	104	27	0.900	0.595
0.90	30	96	27	0.900	0.545
0.94	30	93	27	0.900	0.524

0.96	30	92	27	0.900	0.516
0.98	30	89	27	0.900	0.492
0.99	30	82	27	0.900	0.423

The number of detected regions fell steadily and consistently as the threshold was raised, from 145 detections at a threshold of 0.30 to 82 detections at a threshold of 0.99.. Despite this decline, the True Positive Rate remained fixed at 0.900 across every threshold tested the model continued to correctly identify 27 of the 30 actual birds (90% recall) regardless of how strict the threshold was set is shown in fig 4.3 shown below. This indicates that the 27 true bird detections were associated with strong, high-confidence responses that were never filtered out, while the additional detections being removed as the threshold increased were spurious background responses rather than genuine birds.

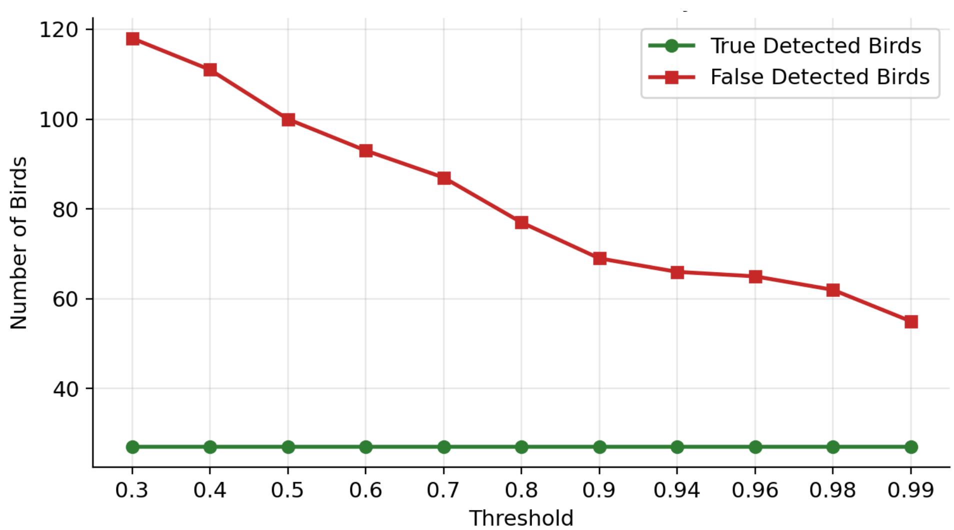

Fig 4.3 Number of true and false detections in GMM model vs the threshold

Because the true detections were unaffected while the total detection count fell, the False Positive Rate decreased monotonically with threshold, from 0.739 at threshold 0.30 down to 0.423 at threshold 0.99 as shown in fig 4.4. This is the most desirable trend a threshold sweep can show: raising the threshold suppressed false alarms without any corresponding loss in recall. On this basis, threshold 0.99 represents the optimum operating point for the GMM model within the range tested, as it minimises the false positive rate (0.423) while preserving the maximum True Positive Rate (0.900) achieved by the model

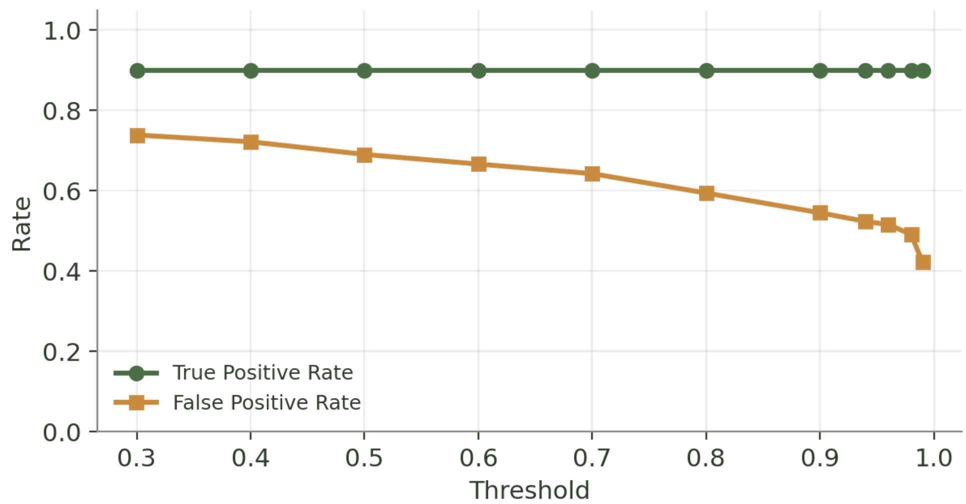

Fig 4.4 True Positive Rate and False Positive Rate of GMM model vs threshold

4.1.2 K-Nearest Neighbour (KNN) Optimization

The KNN model was tested at eleven threshold values ranging from 0.30 to 0.99, matching the range used for the GMM model. The KNN model detection performance across thresholds were shown in table 4.2.

Fig 4.5 Optimisation of KNN

Table 4.2 KNN model detection performance across thresholds

Threshold	Actual No. of Birds	Detected No. of Birds	True Detected Birds	True Positive Rate	False Positive Rate
0.30	30	348	23	0.767	0.906
0.40	30	348	23	0.767	0.906
0.50	30	348	23	0.767	0.906
0.60	30	348	23	0.767	0.906
0.70	30	348	23	0.767	0.906
0.80	30	348	23	0.767	0.906
0.90	30	348	23	0.767	0.906
0.94	30	348	23	0.767	0.906
0.96	30	348	23	0.767	0.906
0.98	30	348	23	0.767	0.906
0.99	30	348	23	0.767	0.906

Unlike the GMM model, the KNN model returned identical results at every threshold tested: 348 candidate regions were detected at each of the eleven thresholds, of which only 23 corresponded to actual birds. This produced a constant True Positive Rate of 0.767 (23 of 30 birds correctly detected) and a constant False Positive Rate of 0.906 across the entire 0.30–0.99 range from fig 4.6 &fig 4.7.

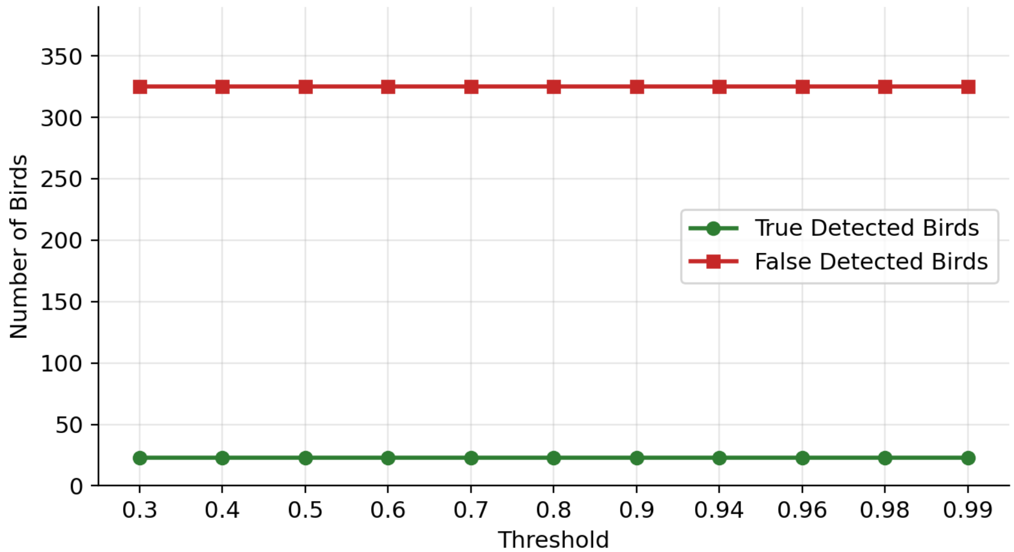

Fig 4.6 True detected and false detected birds in KNN model vs. threshold.

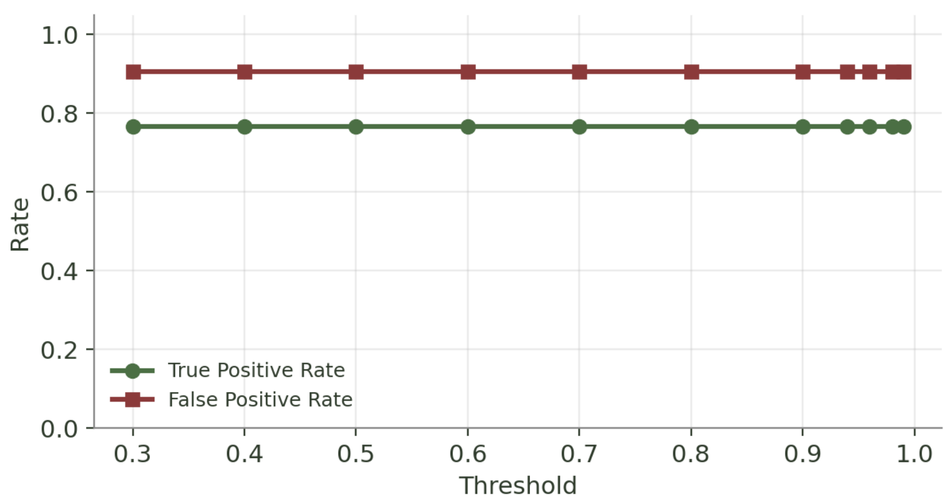

Fig 4.7 True Positive Rate and False Positive Rate of the KNN model vs threshold

As shown in fig 4.8, the true and false detection counts for KNN AND GMM across all threshold values. The complete absence of variation suggests that, within the range examined, the threshold parameter has little to no influence on the KNN background subtractor's output for this footage the model's sensitivity is likely being governed by other internal parameters (such as the number of neighbours, k, or the history/learning-rate settings of the subtractor) rather than the decision threshold itself. The very high False Positive Rate (0.906) also indicates that the KNN model is substantially more prone to misclassifying background motion, lighting changes, or foliage movement as bird detections than the GMM model, returning more than ten spurious detections for every genuine bird identified.

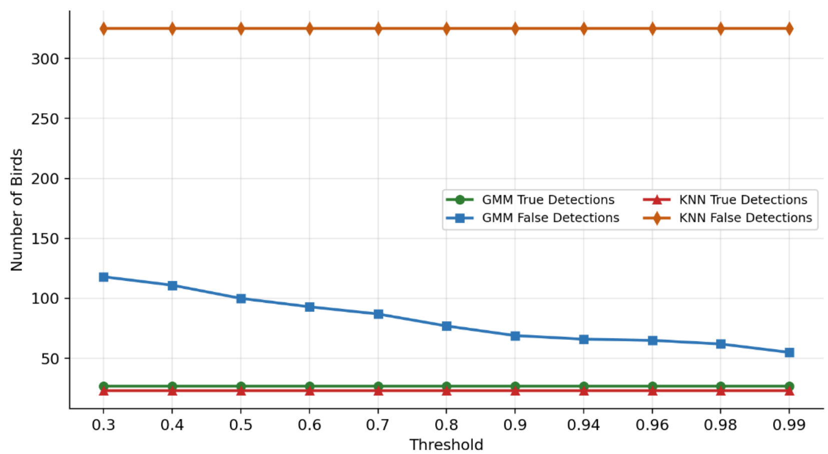

Fig 4.8 True and false detections for GMM and KNN across all threshold

4.1.3 Comparison of Models and Selection of Optimum Configuration

Across every threshold tested, the GMM model outperformed the KNN model on both evaluation metrics. The GMM achieved a higher True Positive Rate (0.900 vs. 0.767), meaning it recovered a larger proportion of the actual birds present, while simultaneously returning far fewer false alarms once the threshold was raised its False Positive Rate fell as low as 0.423, compared with the KNN model's constant 0.906 from fig 4.9. In practical terms, the GMM model at its best threshold flagged 82 candidate regions to find 27 real birds, whereas the KNN model flagged 348 candidate regions to find only 23 real birds roughly half as many useful detections for nearly twice the number of candidates that have to be manually filtered or post-processed.

The GMM model is therefore selected as the better-performing model for this detection task, operated at a threshold of 0.99, since this configuration jointly maximises recall and minimises the false positive burden within the tested range. The KNN model's complete insensitivity to threshold suggests it is not threshold tunable for this application and would require adjustment of its other internal parameters (e.g., the neighbour count or background history length) before it could be considered competitive with the GMM approach.

It should be noted that even the best case GMM result still carries a relatively high False Positive Rate (0.423), so a substantial fraction of detections remain spurious. Future refinement for example, applying morphological filtering, minimum blob-size constraints, or temporal consistency checks on the GMM output could further reduce false detections without comproising the recall achieved at the optimum threshold..

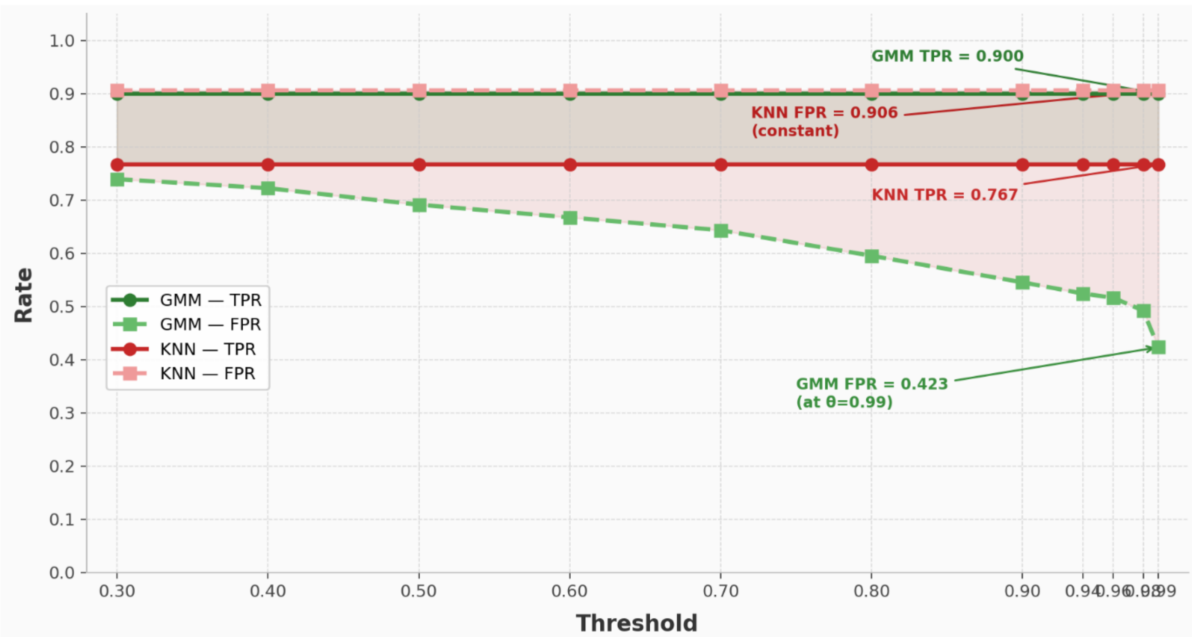

Fig 4.9 TPR and FPR for GMM and KNN across all thresholds.

4.2 DETERRENCE EFFECTIVENESS COMPARISON OF CONVENTIONAL METHOD AND BIRD DETERRENT SYSTEM

To evaluate the effectiveness of the developed UAV based bird deterrence system , structured field observation study was conducted over a total of six observation days, divided equally between the two methods under comparison.

In the first phase, the conventional manual scaring method , comprising shouting, hand clapping, and physical waving by a field worker , was tested over three consecutive days.

Observations were recorded during two sessions each day: early morning and evening, corresponding to the peak bird activity periods in agricultural fields. This yielded a total of six observation sessions for the conventional method.

In the second phase, the developed bird deterrent system, consisting of a manually piloted drone equipped with a GMM-based ESP32-CAM bird detection unit and a drone mounted buzzer activated wirelessly upon detection, was deployed under identical field conditions over another three consecutive days, again with morning and evening sessions, yielding six observation sessions for the proposed system.

In each session, birds were allowed to settle and forage naturally in the field. Once a sufficient flock was observed, the respective deterrence method was activated and the bird return time, defined as the duration (in minutes) from the moment the birds left the field after scaring until they returned, was recorded as the primary performance metric. A longer bird return time signifies a more effective and sustained deterrence.

Table 4.3 Observed Bird Return Time - Conventional vs bird deterrent system

Day	**Session**	**Conventional (min)**	**bird deterrent system (min)**
Day 1	Morning	3.32	20.00
Day 1	Evening	3.20	18.00
Day 2	Morning	3.00	18.00
Day 2	Evening	2.00	16.00
Day 3	Morning	3.45	15.00
Day 3	Evening	3.00	15.00
Mean ± SD	—	**2.99 ± 0.52**	**17.00 ± 2.00**

The observed bird return time for the conventional method ranged from 2.00 to 3.45 min, with a mean value of 2.99 ± 0.52 min from table 4.3. In contrast, the bird deterrent system recorded bird return times ranging from 20.00 to 15.00 min, with a mean value of 17.00 ± 2.00 min. The significantly higher bird return time obtained with bird deterrent system indicates that birds remained away from the field for a longer duration, demonstrating superior deterrence performance compared with the conventional manual scaring method.

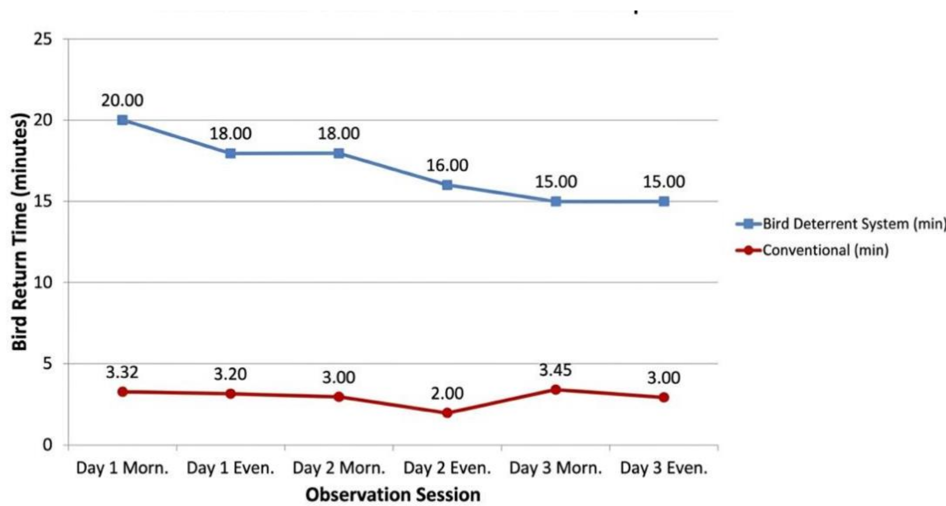

Fig 4.10. Bird return time (minutes) for all six observation sessions

Although slight variations were observed between different sessions, the bird deterrent system consistently provided longer bird return times as in fig 4.10. Therefore, the developed UAV based bird deterrence system proved to be more effective and reliable in reducing bird activity in agricultural fields.

Overall, the bird deterrent system increased the average bird return time by approximately 5.7 times compared with the conventional method, confirming its enhanced deterrence effectiveness.

4.3 COST ESTIMATION

The detailed cost analysis of the developed bird detection and drone based deterrent system is provided in Appendix II. The cost of components is given in table 4.4.

Table 4.4 Cost Components Used

ITEM	RATE(Rs.)
Nano drone	5950
ESP32 cam	800
Transmitter and Receiver	144

Arduino Nano	300
Buzzer	20
Miscellaneous	200
TOTAL ESTIMATED COST	7324/-

4.4 FUTURE SCOPE

The developed bird deterrent system can be further enhanced by replacing the current nano drone with a larger autonomous UAV capable of carrying higher payloads, longer lasting power sources, and additional deterrent devices. The integration of solar powered charging systems can improve energy efficiency and reduce dependence on batteries, enabling longer field operation. Future versions may also incorporate distress call playback and advanced acoustic deterrents to increase bird scaring effectiveness. In addition, implementing autonomous GPS based navigation and flight path planning would reduce manual intervention and allow efficient monitoring of extensive crop fields.

Further improvements can focus on enhancing detection accuracy through advanced image-processing techniques, artificial intelligence, and bird species classification.These developments would contribute to making bird deterrent system a more scalable, intelligent, and sustainable solution for agricultural bird management. Replacement of replacing the current ESP32-CAM with a more powerful edge computing platform such as the ESP32-S3 CAM, Raspberry Pi Camera, or similar AI enabled devices to improve processing speed, detection accuracy, and support advanced bird recognition algorithms. The existing battery powered system can also be upgraded to a solar powered energy system, enabling sustainable operation, reduced maintenance, and longer deployment in agricultural fields. In addition, the nano drone can be replaced with a larger autonomous UAV having greater payload capacity, allowing the integration of larger batteries, more powerful acoustic deterrents, additional sensors, and GPS based autonomous navigation. The deployment of multiple sensor nodes across large agricultural fields.Long term field trials and the incorporation of advanced AI based bird species identification can further enhance the effectiveness, scalability, and practical adoption of the developed bird deterrent system .

CHAPTER V

SUMMARY AND CONCLUSION

Bird depredation is a major challenge in Kerala's paddy cultivation, particularly during the heading and grain filling stages, where species such as the Baya Weaver (Ploceus philippinus) can cause significant crop losses. Conventional bird scaring methods, including scarecrows, reflective materials, firecrackers, and manual patrolling, often lose effectiveness as birds gradually become habituated to these repetitive stimuli. Additionally, the increasing scarcity and cost of agricultural labour have created a need for automated and efficient bird deterrent systems. To address this problem, an integrated bird deterrent system named bird deterrent system was developed. The system combines an ESP32-CAM based bird detection unit with a nano drone-mounted acoustic deterrent. The ground station consists of an ESP32-CAM with an OV3660 camera sensor, a 433 MHz RF transmitter, and Telegram based farmer notification, while the drone station includes a nano drone, Arduino Nano, RF receiver, and piezoelectric buzzer powered by a CR2032 battery. Wireless communication between the two stations enables automatic activation of the deterrent mechanism upon bird detection.

Bird detection was implemented using two background subtraction techniques: Gaussian Mixture Model (GMM) and K-Nearest Neighbours (KNN). Both algorithms were evaluated using a dataset containing 30 confirmed bird occurrences across threshold values ranging from 0.30 to 0.99. The GMM algorithm consistently detected 27 out of 30 birds, achieving a True Positive Rate (TPR) of 0.900, while its False Positive Rate (FPR) decreased from 0.739 to 0.423 as the threshold increased. In contrast, the KNN algorithm achieved a lower TPR of 0.767 and a high FPR of 0.906, showing little responsiveness to threshold variation. Based on these results, GMM with a threshold value of 0.99 was selected as the optimum configuration for field deployment. The effectiveness of bird deterrent system was evaluated through six observation sessions conducted over three consecutive days and compared with conventional manual bird scaring methods. Bird return time, defined as the duration between scaring and re entry of birds into the field, was used as the performance indicator. The conventional method achieved an average return time of 2.99 ± 0.52 minutes, whereas bird deterrent system achieved an average return time of 17.00 ± 2.00 minutes, representing a 5.7-fold improvement in deterrence effectiveness. The superior performance of bird deterrent system is attributed to the drone-mounted buzzer, which delivers an acoustic stimulus from a moving and elevated platform, creating a stronger perception of predation risk than static ground based deterrents. The integration of real time Telegram notifications further enhances practical usability by informing farmers of bird intrusion events remotely. Developed using low cost and readily available components, bird deterrent system provides an affordable, automated, and effective solution for protecting agricultural crops from bird damage while reducing dependence on manual labour.

The bird deterrent system successfully achieved its design objectives of integrating real time bird detection, immediate farmer alert, and automated acoustic deterrence within a single low cost, field deployable system. The Gaussian Mixture Model proved to be the superior detection algorithm for this application, achieving a True Positive Rate of 0.900 while demonstrating meaningful threshold tunability that allows progressive suppression of false positives. At the optimum threshold of 0.99, the GMM achieved the best balance of recall and precision, and was selected for operational deployment in the bird deterrent system. The KNN algorithm, despite its theoretical flexibility, showed no threshold responsiveness under field conditions and generated a False Positive Rate of 0.906, making it unsuitable for this application without further parameter tuning.

The bird deterrent system achieved a mean bird deterrence duration of 17.00 ± 2.00 minutes per activation, representing a 5.7-fold improvement over the mean of 2.99 ± 0.52 minutes achieved by conventional manual scaring. This difference remained consistent across all six evaluation sessions, demonstrating the reliability and repeatability of the system's deterrence performance under real field conditions.

The integration of Telegram-based real-time farmer notification with the detection event provides meaningful operational value, enabling remote crop monitoring without requiring constant physical presence at the field. This feature is particularly relevant given the rising cost and scarcity of agricultural labour in Kerala and has potential to significantly reduce the labour burden associated with bird management during the critical grain filling stage.

The aerial delivery of acoustic deterrence from the drone platform, operating from an unpredictable and elevated position, is identified as the key factor distinguishing bird deterrent system’s performance from conventional static or ground-based deterrent methods. Moving acoustic sources have been consistently demonstrated in the literature to produce substantially lower habituation rates than stationary sources emitting identical stimuli, and the field results obtained in this study are consistent with that body of evidence.

The prototype confirms the practical feasibility of deploying integrated IoT-UAV bird deterrent systems at the farm level in Kerala using commercially available, low cost hardware. The total system cost remains within a range accessible to small and marginal farmers, and the operational simplicity requiring only smartphone based monitoring and periodic drone deployment makes the technology suitable for real world adoption without specialised technical training.

Future work should address the residual False Positive Rate in the GMM detection output through the application of morphological filtering, minimum contour-size constraints, and temporal consistency checks on detection events. Integration of distress call playback in the bird-sensitive 1–4 kHz frequency range as an additional acoustic deterrent modality on the drone, and incorporation of autonomous patrol flight path programming, would further enhance the system's deterrence efficacy and reduce reliance on manual drone operation. Long term field trials spanning multiple crop seasons and covering larger field areas would provide the empirical evidence required to quantify seasonal deterrence effectiveness and to validate the system's economic benefit in terms of yield protection value relative to system cost.

In conclusion, bird deterrent system represents a viable, scalable, and farmer accessible solution to a longstanding agricultural problem in Kerala. Its development demonstrates that advances in embedded computing, computer vision, wireless communication, and consumer drone technology can be effectively combined to deliver precision agricultural tools that address real and economically significant challenges faced by smallholder paddy farmer.

CHAPTER VI

REFERENCES

Aloysius, N. and Geetha, M. 2017. A review of deep learning architectures for computer vision. *International Journal of Advanced Research in Computer Science*. 8(5): 577–580.

Altman, N.S. 1992. An introduction to kernel and nearest-neighbor nonparametric regression. *The American Statistician*. 46(3): 175–185.

Arduino. 2023. *ATmega328P Microcontroller Datasheet*. Microchip Technology Inc., Chandler, AZ, USA.

Auffray, J.C., Boutin, J.M. and Le Louarn, H. 1994. Effectiveness of conspecific distress calls for reducing House Sparrow (*Passer domesticus*) damage in wheat fields. *Crop Protection*. 13(7): 495–500.

Bhusal, S., Khanal, K., Goel, S., Karkee, M. and Taylor, M.E. 2019. Bird deterrence in a vineyard using an unmanned aerial system (UAS). *Transactions of the ASABE*. 62(2): 561–569.

Bishop, J., McKay, H., Parrott, D. and Allan, J. 2003. Review of International Research Literature Regarding the Effectiveness of Auditory Bird Scaring Techniques and Potential Alternatives. Central Science Laboratory, Department for Environment, Food and Rural Affairs (DEFRA), London, UK. 53.

Blackwell, B.F., Fernández-Juricic, E., Seamans, T.W. and Dolbeer, R.A. 2012. Use of green lasers for dispersing birds. *Human–Wildlife Interactions*. 6(2): 197–204.

Bomford, M. and O'Brien, P.H. 1990. Sonic deterrents in animal damage control: A review of device tests and effectiveness. *Wildlife Society Bulletin*. 18(4): 411–422.

Boominathan, V. and others. 2014. Bird species identification using convolutional neural networks and Mel-frequency cepstral coefficients. *Pattern Recognition Letters*. 48: 94–101.

Boukoberine, M.N., Zhou, Z. and Benbouzid, M. 2019. Power supply technologies for unmanned aerial vehicles: A review. *IEEE Access*. 7: 78333–78344.

Boyle, D. and others. 2014. Wireless charging system for autonomous UAV battery replenishment. *IEEE Transactions on Power Electronics*. 29(12): 6409–6419.

Bradski, G. and Kaehler, A. 2008. *Learning OpenCV*. O'Reilly Media, Sebastopol, CA, USA.

Brambilla, M., Ferrante, E., Birattari, M. and Dorigo, M. 2013. Swarm robotics: A review from the swarm engineering perspective. *Swarm Intelligence*. 7(1): 1–41.

Brown, R.N. and Brown, D.H. 2021. Robotic laser scarecrows: A tool for controlling bird damage in sweet corn. *Crop Protection*. 146: 105652.

Choudhary, A. and others. 2017. Recent advances in lithium-ion and lithium-polymer batteries for UAV applications. *Journal of Power Sources*. 342: 70–83.

Conover, M.R. 2002. *Resolving Human–Wildlife Conflicts: The Science of Wildlife Damage Management*. CRC Press, Boca Raton, FL, USA.

Conover, M.R. and Dolbeer, R.A. 2007. Use of frightening devices and repellents to reduce bird damage to agricultural crops. USDA National Wildlife Research Center – Human–Wildlife Conflicts Monograph. 1–24.

Cover, T.M. and Hart, P.E. 1967. Nearest neighbor pattern classification. *IEEE Transactions on Information Theory*. 13(1): 21–27.

Crupi, V. and others. 2025. Autonomous nano-UAV fleet for vineyard pest detection using low-power onboard artificial intelligence. *IEEE Robotics and Automation Letters*. 10(1): 1–8.

Cuthill, I.C., Partridge, J.C., Bennett, A.T.D., Church, S.C., Hart, N.S. and Hunt, S. 2000. Ultraviolet vision in birds. *Advances in the Study of Behavior*. 29: 159–214.

Dalal, N. and Triggs, B. 2005. Histograms of oriented gradients for human detection. Proc. IEEE Conference on Computer Vision and Pattern Recognition (CVPR): 886–893.

Dantu, K. and others. 2011. Energy-aware task allocation for long-term multi-UAV surveillance. Proc. IEEE International Conference on Robotics and Automation (ICRA): 1940–1945.

DJI. 2022. *Mini Series Drone User Manual and Technical Specifications*. DJI Technology Co., Ltd., Shenzhen, China.

Dolbeer, R.A., Wright, S.E., Cleary, E.C. and Seubert, J.L. 2000. Wildlife strikes to civil aircraft in the United States, 1990–1998. Federal Aviation Administration, Office of Airport Safety and Standards, Serial Report No. 6.

Dunbabin, M. and Marques, L. 2012. Robots for environmental monitoring: Significant advancements and applications. *IEEE Robotics & Automation Magazine*. 19(1): 24–39.

Elser, J.L., Anderson, A., Lindell, C.A. and others. 2016. Economic impacts of bird damage and management in U.S. sweet cherry production. *Crop Protection*. 83: 9–14.

Espressif Systems. 2023. *ESP32-CAM Technical Reference Manual*. Espressif Systems, Shanghai, China.

Feare, C.J. 1980. The economics of Starling damage. In: Wright, E.N. (Ed.), *Bird Problems in Agriculture*. 39–55.

Floreano, D. and Wood, R.J. 2015. Science, technology and the future of small autonomous drones. *Nature*. 521(7553): 460–466.

Galceran, E. and Carreras, M. 2013. A survey on coverage path planning for robotics. *Robotics and Autonomous Systems*. 61(12): 1258–1276.

Gorenzel, W.P., Salmon, T.P. and Marcum, D.B. 1994. Evaluation of alarm calls and raptor effigies for dispersing American Crows in orchards. *Crop Protection*. 13(6): 435–442.

Hagstrum, J.T. 2000. Infrasound and the avian navigational map. *Journal of Experimental Biology*. 203(7): 1103–1111.

Hassanalian, M. and Abdelkefi, A. 2017. Classifications, applications, and design challenges of drones: A review. *Progress in Aerospace Sciences*. 91: 99–131.

Howard, A.G., Zhu, M., Chen, B. and others. 2017. MobileNets: Efficient convolutional neural networks for mobile vision applications. arXiv preprint arXiv:1704.04861.

Jeong, S. and others. 2013. Piezoelectric vibration energy harvesting for quadrotor UAV landing gear. *Smart Materials and Structures*. 22(9): 095017.

Jocher, G., Chaurasia, A. and Qiu, J. 2022. YOLOv5 by Ultralytics. GitHub Repository.

Keennon, M., Klingebiel, K. and Won, H. 2012. Development of the Nano Hummingbird: A tailless flapping-wing micro air vehicle. 50th AIAA Aerospace Sciences Meeting. AIAA 2012-0588.

Kendoul, F. 2012. Survey of advances in guidance, navigation, and control of unmanned rotorcraft systems. *Journal of Field Robotics*. 29(2): 315–378.

Khan, M., Ahmed, S. and Ali, R. 2020. Bird classification in agricultural fields using K-nearest neighbour algorithm. *International Journal of Advanced Computer Science and Applications*. 11(8): 245–252.

Kross, S.M., Tylianakis, J.M. and Nelson, X.J. 2012. Effects of introducing falcons into vineyards on bird damage. *Conservation Biology*. 26(5): 935–943.

Lim, R. and others. 2012. Reactive obstacle avoidance for quadrotors using time-of-flight sensors. Proc. IEEE/RSJ International Conference on Intelligent Robots and Systems: 197–204.

Lowe, D.G. 2004. Distinctive image features from scale-invariant keypoints. *International Journal of Computer Vision*. 60(2): 91–110.

Madsen, J. 1998. Experimental refuges for migratory waterfowl in Danish wetlands. *Journal of Applied Ecology*. 35: 398–417.

Manz, S.T., Sieving, K.E., Brown, R.N., Klug, P.E. and Kluever, B.M. 2024. Experimental assessment of laser scarecrows for reducing avian damage to sweet corn. *Pest Management Science*. 80(3): 1547–1556.

Mellinger, D. and Kumar, V. 2011. Minimum snap trajectory generation and control for quadrotors. Proc. IEEE International Conference on Robotics and Automation: 2520–2525.

Meng, Q., Zhang, Y. and Li, H. 2019. Development of an autonomous directional acoustic bird deterrent system using computer vision. *Computers and Electronics in Agriculture*. 162: 482–491.

Nifong, J.C., Sumners, J.A. and Hartup, B.K. 2015. Effectiveness of distress-call playback in dispersing nuisance bird flocks. *Wildlife Society Bulletin*. 39(2): 321–329.

Notter, B. and others. 2016. Autonomous UAV-based bird deterrence in agricultural fields using onboard vision. *Computers and Electronics in Agriculture*. 127: 662–670.

Osenberg, C.W., Sarnelle, O., Cooper, S.D. and Holt, R.D. 1999. Resolving ecological questions through meta-analysis. *Ecology*. 80(4): 1105–1117.

Pimentel, D., Zuniga, R. and Morrison, D. 2005. Update on the environmental and economic costs associated with alien-invasive species in the United States. *Ecological Economics*. 52(3): 273–288.

Poot, H., Ens, B.J., de Vries, H., Donners, M.A.H., Wernand, M.R. and Marquenie, J.M. 2008. Green light for nocturnally migrating birds. *Ecology and Society*. 13(2): 47.

Quigley, M. and others. 2010. ROS: An open-source Robot Operating System. ICRA Workshop on Open Source Software: 1–6.

Redmon, J. and Farhadi, A. 2018. YOLOv3: An incremental improvement. arXiv preprint arXiv:1804.02767.

Redmon, J., Divvala, S., Girshick, R. and Farhadi, A. 2016. You Only Look Once: Unified, real-time object detection. Proc. IEEE Conference on Computer Vision and Pattern Recognition (CVPR): 779–788.

Rosten, E. and Drummond, T. 2006. Machine learning for high-speed corner detection. Proc. European Conference on Computer Vision (ECCV): 430–443.

Rublee, E., Rabaud, V., Konolige, K. and Bradski, G. 2011. ORB: An efficient alternative to SIFT or SURF. Proc. IEEE International Conference on Computer Vision (ICCV): 2564–2571.

Ruzvidzo, M. 2022. Design and development of a bird detection and deterring system using UAV technology. Capstone Project Report.

Sandler, M., Howard, A., Zhu, M. and others. 2018. MobileNetV2: Inverted residuals and linear bottlenecks. Proc. IEEE Conference on Computer Vision and Pattern Recognition (CVPR): 4510–4520.

Seamans, T.W. 2004. Response of roosting blackbirds to a bioacoustic harassment system. *Wildlife Society Bulletin*. 32(3): 746–751.

Singh, A., Kumar, P. and Sharma, V. 2018. Motion-based pest and bird monitoring using Gaussian mixture models. *International Journal of Agricultural and Biological Engineering*. 11(4): 120–127.

Spagnolo, P. and others. 2021. Deep learning for bird monitoring: A review. *Ecological Informatics*. 61: 101236.

Srivastava, A. and others. 2022. Lightweight YOLOv5-based bird detection for agricultural UAV applications. *Computers and Electronics in Agriculture*. 196: 106873.

Stauffer, C. and Grimson, W.E.L. 1999. Adaptive background mixture models for real-time tracking. Proc. IEEE Conference on Computer Vision and Pattern Recognition (CVPR). 2: 246–252.

Tracey, J., Bomford, M., Hart, Q., Saunders, G. and Sinclair, R. 2007. *Managing Bird Damage to Fruit and Other Horticultural Crops*. Bureau of Rural Sciences, Canberra, Australia.

Tracey, J.P., Bomford, M., Hart, Q., Saunders, G. and Sinclair, R. 2007. *Managing Bird Damage to the Rice Industry*. Bureau of Rural Sciences, Canberra, Australia.

van Dijk, J.G.B. and others. 2019. BirdScan-MR1: Doppler radar system for bird detection and classification. *Ecological Informatics*. 52: 33–42.

Viola, P. and Jones, M. 2001. Rapid object detection using a boosted cascade of simple features. Proc. IEEE Conference on Computer Vision and Pattern Recognition (CVPR): 511–518.

Voigt, C.C. and others. 2012. Hearing abilities of European birds determined using auditory brainstem response measurements. *Journal of Comparative Physiology A*. 198(12): 889–900.

Wang, X. and others. 2020. Thermal management of lithium-polymer batteries for unmanned aerial vehicles. *Journal of Energy Storage*. 31: 101665.

Wang, Y., Zhang, X. and Liu, H. 2019. Computer vision-based moving raptor decoy system for bird deterrence. *Computers and Electronics in Agriculture*. 158: 293–302.

Wang, Z. and Wong, K.C. 2018. Autonomous bird deterrent system for vineyards using multiple bio-inspired unmanned aerial vehicles. 10th International Micro-Air Vehicles Conference (IMAV 2018).

Zivkovic, Z. 2004. Improved adaptive Gaussian mixture model for background subtraction. Proc. International Conference on Pattern Recognition. 2: 28–31.

Zivkovic, Z. and Van Der Heijden, F. 2006. Efficient adaptive density estimation per image pixel for background subtraction. *Pattern Recognition Letters*. 27(7): 773–780.

APPENDIX-I

```
#include "esp_camera.h"

#define SCALE 0.25
#define GMM_COMPONENTS 4

int FIELD_START;
int birdCount = 0;

struct Detection
{
    int x1;
    int y1;
    int x2;
    int y2;
    int area;
};

void setup()
{
    Serial.begin(115200);

    initCamera();
    initWiFi();
    initTelegram();
    initRF();
}

void loop()
{
    camera_fb_t *fb = esp_camera_fb_get();

    if(fb == NULL)
    {
        Serial.println("Capture Failed");
        return;
    }

    Image img = decodeJPEG(fb);

    birdCount = detectBirdsGMM(img);

    Serial.print("Bird Count : ");
    Serial.println(birdCount);
```

```
    if(birdCount >= 3)
    {
        sendTelegram("Birds Detected");

        delay(10000);

        sendRF("BIRD");
    }

    esp_camera_fb_return(fb);

    delay(3000);
}

int detectBirdsGMM(Image image)
{
   FIELD_START = image.height * 0.52;

   Image field = cropImage(image,
                           0,
                           FIELD_START,
                           image.width,
                           image.height);

   Image resized = resize(field,SCALE);

   Matrix gray = convertGray(resized);

   Matrix bgLarge = gaussianBlur(gray,41);

   Matrix bgSmall = gaussianBlur(gray,9);

   Matrix DoG = bgLarge - bgSmall;

   Matrix red = getRed(resized);

   Matrix green = getGreen(resized);

   Matrix blue = getBlue(resized);

   normalize(red);

   normalize(green);

   normalize(blue);

   normalize(gray);

   normalize(DoG);

   FeatureVector features;

   for(each pixel)
   {
```

```
        Feature f;

        f.r = red(pixel);

        f.g = green(pixel);

        f.b = blue(pixel);

        f.gray = gray(pixel);

        f.dog = DoG(pixel) * 3;

        features.push_back(f);
    }
gmm.components = 4;

gmm.train(features);

LabelMap labels;

ProbabilityMap probability;

labels = gmm.predict(features);

probability = gmm.predictProbability(features);

int birdComponent = findComponentWithHighestDoG(gmm);

BinaryMask mask;

for(each pixel)
{
    bool prob = probability(pixel,birdComponent) > 0.55;

    bool dark = gray(pixel) < 0.30;

    bool dog = DoG(pixel) > 0.05;

    if(prob && dark && dog)
        mask(pixel)=1;
    else
        mask(pixel)=0;
}
  morphologyOpen(mask);

  morphologyClose(mask);

  Blob blobs[100];

  int totalBlobs = connectedComponents(mask,blobs);
```

```
    int totalBlobs = connectedComponents(mask,blobs);

    Detection birds[100];

    int totalBirds = 0;

    for(int i=0;i<totalBlobs;i++)
    {
        if(blobs[i].area>=2 &&
           blobs[i].area<=50)
        {
          if(blobs[i].aspectRatio<4.0)
          {
              birds[totalBirds++] = blobs[i];
          }
        }
    }

    drawBoundingBoxes(image,birds,totalBirds);

    return totalBirds;
}void setup() {
  // put your setup code here, to run once:

}

void loop() {
  // put your main code here, to run repeatedly:

}
```

APPENDIX-II

COST ESTIMATION

1. Cost of Fabrication

Sl. No.	Item	Quantity	Price (₹)
1	Nano toy drone	1 No	6,000
2	Li-coin battery	2 Nos (₹20 each)	40
3	ESP32-CAM module	1 No	800
4	RF Transmitter & Receiver	1 set	144
5	Arduino Nano	1 No	300
6	Miscellaneous (wiring, connectors, mounting)	—	200
	Total Cost, ₹		7,484

2. Assumptions and Operating Parameters

Parameter	Value
Initial fabrication cost (P)	₹7,484
Salvage value (S, 10%)	₹748

Economic life (L)	2 years
Battery flight time	15 min/charge
Battery charging time	30 min
Duty cycle (flight ÷ (flight+charge))	1/3
Bird active window	6 h/day (6–10 AM, 4–6 PM)
Effective flying time	2 h/day
Operating days/year (sowing + harvesting, 2 seasons)	60 days/year
Annual working hours	120 h/year
Interest rate (i)	10%
Repair & maintenance	6% of P/year
Shelter, taxes & insurance	2% of P/year
Electricity tariff	₹8/kWh
Battery charger power	5 W
ESP32-CAM power (continuous)	2.5 W
Labour (if hired operator)	₹700/day; assumed ₹0 if farmer self-operated
Area protected per unit	5 acres
Paddy yield, Kerala average	1,130 kg/acre/season

Cropping seasons/year	2
Paddy price (2025–26 MSP basis)	₹24/kg (≈ ₹2,369/quintal)
Bird damage without deterrent	5% of yield (literature range 0.2–15%)
Deterrent effectiveness	80% reduction in damage

3. Economic Analysis of the Bird Deterrent and Detection Drone

3.1 Fixed Cost

Depreciation

$$D = (7{,}484 - 748) / 2 = ₹3{,}368/\text{year}$$

Interest

$$I = ((7{,}484 + 748)/2) \times 0.10 = ₹412/\text{year}$$

Shelter, Taxes & Insurance

$$STI = 0.02 \times 7{,}484 = ₹150/\text{year}$$

Total Fixed Cost = 3,368 + 412 + 150 = ₹3,930/year = ₹32.74/h

3.2 Operating Cost

Electricity (charging) = 0.005 kW × (30/45) × ₹8/kWh ≈ ₹0.03/h

Labour = ₹0/h (farmer self operated base case)

Repair & Maintenance = (0.06 × 7,484) / 120 = ₹3.74/h

Total Operating Cost = 0.03 + 0 + 3.74 = ₹3.77/h

3.3 Total Cost of Operation

TC = Fixed Cost/h + Operating Cost/h = 32.74 + 3.77 = ₹36.51/h

3.4 Continuous Monitoring Cost (ESP32-CAM)

Energy = 0.0025 kW × 24 h × 365 days = 21.9 kWh/year

Monitoring Cost = 21.9 × ₹8 = ₹175/year

3.5 Annual Operating Expense

Flight operation expense = 36.51 × 120 = ₹4,381/year

Annual Expense = 4,381 + 175 = ₹4,556/year

3.6 Annual Value of Crop Protected

Annual production = 5 acres × 1,130 kg/acre × 2 seasons = 11,300 kg/year

Crop value = 11,300 × ₹24 = ₹2,71,200/year

Potential loss without deterrent (5%) = ₹13,560/year

Annual Benefit = 13,560 × 0.80 (deterrent effectiveness) = ₹10,848/year

3.7 Annual Net Benefit

Net Benefit = 10,848 − 4,556 = ₹6,292/year

3.8 Benefit–Cost Ratio

B:C Ratio = 10,848 / 4,556 = 2.38

3.9 Break-even Point

Variable cost per acre-season = (3.77 × 120 + 175) / 10 = ₹62.76/acre-season

Benefit per acre-season = 10,848 / 10 = ₹1,084.80/acre-season

Contribution = 1,084.80 − 62.76 = ₹1,022.04/acre-season

BEP = 3,930 / 1,022.04 = 3.85 acre-seasons/year

The unit is operated over 10 acre-seasons/year (5 acres × 2 seasons); break-even is therefore reached well within the first season.

3.10 Payback Period

Payback Period = 7,484 / 6,292 ≈ 1.19 years ≈ 14 months

Summary

Parameter	**Value**
Fixed cost	₹32.74/h (₹3,930/year)
Operating cost	₹3.77/h
Total cost of operation	₹36.51/h
Continuous monitoring cost	₹175/year
Annual operating expense	₹4,556/year
Annual benefit (crop protected)	₹10,848/year
Annual net benefit	₹6,292/year
Benefit–cost ratio	2.38
Break-even point	3.85 acre-seasons/year
Payback period	≈ 1.19 years (14 months)

DEVELOPMENT OF A BIRD DETECTION AND DRONE BASED DETTERENT SYSTEM

BY

APARNA K (2022-02-043)

ALEESHA K S (2022-02-048)

HIBA K V (2021-02-026)

ABSTRACT

Submitted in partial fulfilment of the requirement for the degree of

BACHELOR OF TECHNOLOGY IN AGRICULTURAL ENGINEERING

Faculty of Agricultural Engineering and Technology

Kerala Agricultural University

DEPARTMENT OF FARM MACHINERY AND POWER ENGINEERING

KELAPPAJI COLLEGE OF AGRICULTURAL ENGINEERING AND FOOD TECHNOLOGY

Tavanur-679573, Malappuram

Kerala, India

2026

ABSTRACT

Bird damage to paddy crops represents one of the most persistent and economically significant biotic stressors affecting agricultural productivity in Kerala, particularly during the heading and grain filling stages. The Baya Weaver bird (*Ploceus philippinus*), locally known as Attakili, is among the most destructive avian pests in the paddy growing regions. Conventional bird scaring methods including scarecrows, reflective tapes, gas cannons, and manual patrolling suffer from rapid habituation declining rural agricultural labour availability.

This study presents the prototype development and evaluation of bird deterrent system, an integrated nano drone based bird deterrent system designed for small and marginal paddy farmers in Kerala. The system employs a two station architecture comprising a ground station and a drone mounted deterrent station. The ground station utilises an ESP32-CAM module equipped with an OV3660 image sensor for continuous field surveillance. Bird detection is performed using the Gaussian Mixture Model (GMM) algorithm,Upon detection, the system simultaneously dispatches a real time alert to the farmer's mobile phone via the Telegram notification platform and, after a ten second delay, wirelessly transmits a 433 MHz RF signal to the drone mounted receiver unit. The drone unit, comprising an Arduino Nano microcontroller and a piezoelectric buzzer, activates an acoustic deterrent upon receiving the signal.

Comparative evaluation of GMM and K-Nearest Neighbours (KNN) background subtraction algorithms was performed across eleven probability threshold values (0.30 to 0.99) using a ground truth dataset of 30 bird occurrences. The GMM achieved a consistent True Positive Rate of 0.900 across all thresholds, with the False Positive Rate declining monotonically from 0.739 at threshold 0.30 to 0.423 at threshold 0.99. The KNN model produced a fixed True Positive Rate of 0.767 and an invariant False Positive Rate of 0.906 across all thresholds, indicating threshold insensitivity and substantially higher false alarm generation. GMM operated at threshold 0.99 was selected as the optimum detection configuration. Field deterrence trials over six observation sessions demonstrated that bird deterrent system achieved a mean bird return time of 17.00 ± 2.00 minutes, compared to 2.99 ± 0.52 minutes for conventional manual scaring a 5.7-fold improvement in deterrence duration. The bird deterrent system demonstrates that low cost embedded IoT components, combined with motion based computer vision and aerial acoustic deterrence, can deliver effective, scalable, and farmer accessible bird management for paddy cultivation in Kerala.